

# **Notech™ ventilation solution**

**Investigation of draught in a new sustainable ventilation concept  
for schools**

**Master's Thesis**

**Nicolette Chuda, Lasse Myrrhøj Nielsen, Aleksandra Szewczuk**

The Faculty of Engineering and Science  
Department of the Built Environment  
Thomas Menns Vej 23  
9220 Aalborg, Denmark



Copyright © Aalborg University 2024

This master thesis utilized the following tools and software for gathering and treating data, as well as creating drawings: LabVIEW, Microsoft Excel, Autodesk Revit.



**BUILD**

Aalborg University  
<http://www.aau.dk>

## AALBORG UNIVERSITY

### STUDENT REPORT

**Title:**

Notech™ ventilation solution - investigation of draught in a new sustainable ventilation concept for schools

**Project Period:**

04.09.2023 - 11.01.2024

**Participants:**

Nicolette Chuda  
Lasse Myrrhøj Nielsen  
Aleksandra Anna Szewczuk

**Supervisor:**

Per Kvols Heiselberg

**ECTS:**

30

**Page Numbers:** 46

**Date of Completion:**

10.01.2024

**Abstract:**

This paper is a Master's thesis of the Building Energy Design programme at Aalborg University. It investigates the issue of draught in connection with a new natural ventilation solution - Notech. The study is conducted through a series of systematic experiments in the laboratory setting. The aim of this study is to understand the current performance and limitations of the panel. Moreover, to determine a suitable evaluation method and suggest proposals for improvement based on earlier findings. The results of this investigation hope to provide the developers with a better understanding of the system and its behaviour to be used in optimization of the panel.

*The content of this report is freely available, but publication (with reference) may only be pursued due to agreement with the author. By accepting the request from the fellow student who uploads the study group's project report in Digital Exam System, you confirm that all group members have participated in the project work, and thereby all members are collectively liable for the contents of the report. Furthermore, all group members confirm that the report does not include plagiarism.*





# Preface

The paper presents the investigation into draught in connection with the new sustainable ventilation concept for schools - the Notech panel. The objective of the study is to assist the developers in enhancing their understanding of the Notech panel's performance and to explore potential solutions to address the draught issue through conduction of systematic experiments. This short study provides introduction to the topic, explains the utilized methods and presents the key findings, complemented by supplementary data presented in the appendix.

This master's thesis represents the culmination of efforts undertaken during the fourth semester of the Building Energy Design programme. The project was overseen by Per Kvols Heiselberg and developed in collaboration with Jannick K. Roth from WindowMaster and Carlo Volf from Volfdesign. We express our sincere gratitude to them and other AAU staff for their guidance and support throughout the project. Furthermore, we would like to extend our gratitude to WindowMaster A/S for providing the prototype of the Notech panel, which was a crucial asset.

Aalborg University, January 10, 2024

*Nicolette Chudá*

---

Nicolette Chuda  
nchuda21@student.aau.dk

*Lasse Myrrhøj Nielsen*

---

Lasse Myrrhøj Nielsen  
lnielk21@student.aau.dk

*Aleksandra Anna Szewczuk*

---

Aleksandra Anna Szewczuk  
aszewc21@student.aau.dk



# Summary

The construction industry has in recent times experienced a resurgence of the implementation of natural ventilation in an effort to reduce the carbon emissions and enhance indoor environment. The newly developed natural ventilation system Notech fits into that narrative and has already been incorporated in Feldballe school, among other projects. The pilot study revealed that this solution has 95% lower CO<sub>2</sub> footprint and 65% lower costs than mechanical ventilation systems and its performance is satisfactory throughout most of the year [16]. However, it was observed that there is an issue of draught during low outdoor temperatures. Addressing this issue is a necessary step to optimize both the design of the Notech panel and indoor environment in the school.

This research addresses the issue of draught through a systematic conduction of experiments in the laboratory settings on the prototype. Firstly, the current performance and limits of the Notech panel in regards to air activity in the filter and draught rates using thermographic camera and anemometers are investigated. Based on these findings, possible solutions for improvement of the draught issue are suggested. The evaluated proposals include different types of shelf systems and a heater. Three different draught models (Fanger ISO 7730, Fanger corrected to ankle level and ASHRAE 55:2021) are utilized for evaluation.

The first stage of the measurements shows the impact of airflow and inlet opening on distribution of the air through the panel. These findings contribute to better understanding and can be potentially used for future improvements. In regards to the draught rate, limit for the panel was found at 22 dT, 47 l/s and 33% opening of the inlet. Comparison of the three draught models revealed that Fanger's model from ISO 7730 overestimates the results, as it is developed for the neck area. CBE is not suited for winter conditions due to the limitation on clothing input. This resulted in considering Fanger's model corrected to ankles to be the best suited for evaluation of draught at ankle level. The explored solutions for draught reveal that a heater is most effective at combating draught, however it is the most energy consuming. To minimize the energy usage, this solution was tested in a combination with a shelf system.



# Contents

<b>Preface</b>	<b>v</b>
<b>1 Introduction</b>	<b>1</b>
1.1 Purpose . . . . .	2
1.2 State of art . . . . .	2
1.2.1 Notech natural ventilation panel . . . . .	2
1.2.2 Draught models . . . . .	4
1.3 Problem formulation . . . . .	6
1.3.1 Limitations . . . . .	7
<b>2 Methods</b>	<b>9</b>
2.1 Laboratory setup . . . . .	9
2.2 Measurements procedure and conditions . . . . .	10
2.2.1 Stage 1 . . . . .	11
2.2.2 Stage 2 . . . . .	13
<b>3 Findings</b>	<b>15</b>
3.1 Stage 1 . . . . .	15
3.1.1 Step 1 - thermography . . . . .	15
3.1.2 Step 2 - draught rate . . . . .	18
3.2 Stage 2 - solutions . . . . .	26
3.2.1 Step 1 - inlet design . . . . .	26
3.2.2 Step 2 - heater . . . . .	31
3.2.3 Step 3 - shelves . . . . .	33
3.2.4 Step 4 - combined solution of shelves and heater . . . . .	42
<b>4 Conclusion</b>	<b>45</b>
<b>Bibliography</b>	<b>47</b>

<b>A</b>	<b>Measurements</b>	<b>1</b>
A.1	Conditions . . . . .	1
A.2	Procedure & laboratory setup . . . . .	4
A.3	Equipment . . . . .	9
A.4	Airflow correction . . . . .	10
A.5	Blower door test . . . . .	13
A.6	Notech panel visualisations . . . . .	27
<b>B</b>	<b>Calibration</b>	<b>29</b>
<b>C</b>	<b>Results</b>	<b>41</b>
C.1	Stage 1 step 1 - thermography . . . . .	41
C.2	Stage 1 step 2 - draught rate . . . . .	48
C.2.1	Mean radiant temperature measurement results . . . . .	48
C.2.2	Velocity development . . . . .	50
C.2.3	Temperature development . . . . .	55
C.2.4	Draught models . . . . .	59
C.3	Stage 2 step 1 - inlet design . . . . .	62
C.4	Stage 2 step 2 - heater . . . . .	71
C.5	Stage 2 step 3 - shelves . . . . .	83
<b>D</b>	<b>Raw data - LabView</b>	<b>107</b>

# Chapter 1

## Introduction

The urgent need to address climate change has prompted a universal shift towards sustainable practices, advocating for innovative strategies that not only reduce the carbon footprint but also do not compromise the health, safety, and well-being of people. The building industry is widely acknowledged as pivotal sector that needs to undergo a green transition, as it is responsible for almost 40% of global energy consumption. [5].

In this pursuit for energy-efficient solutions, natural ventilation has arisen as a promising and integral element of sustainable building design. Natural ventilation relies on principle of temperature and pressure difference to improve the indoor air quality and to regulate indoor temperatures. Despite being an antiquated concept, currently it experiences resurgence as a forward-thinking strategy that allows for reduction of carbon emissions and enhancement of the indoor environment. [17]

The buildings used for education, could benefit from the potential of natural ventilation. They possess a significant need for sufficient ventilation, as too high temperatures or CO<sub>2</sub> concentration, will result in reduced performance of the students. In fact their performance can decrease by 10% if the CO<sub>2</sub> concentration reaches 1600 ppm. The indoor climate in schools is currently maintained primarily through the use of mechanical operated ventilation system, which therefore entails costs in the form of maintenance of the system and energy consumption. [16] [13]

In that regard, the newly developed natural ventilation-based system, Notech, a collaborative effort by WindowMaster, Volfdesign, and the Technological Institute, seamlessly integrates into the narrative. The pilot study revealed that the Notech solution, due to deliberate materials selection and thoughtful design, can achieve 95% lower CO<sub>2</sub> footprint than traditional mechanical systems, while also amounting to 65% lower installation and operational costs. [16]

## 1.1 Purpose

The Notech panel has been incorporated in buildings across Denmark, including Feldballe school where four Notech panels are used as a sole ventilation system in a newly built annex. According to the reports from school employees and pupils, the prototype shows promising results in its ability to provide sufficient fresh air. Despite the overall satisfaction with the ventilation system, there has been complaints about draught during periods with low outdoor temperatures. These claims have been confirmed by the Technological Institute. In their report, the measurements on draught show significantly high rates in the zone near the panel.

The Notech ventilation strategy is based on buoyancy – the air is driven to the room by temperature difference. When the outdoor temperature is lower than the indoor temperature, the incoming air drops to the floor due to gravity, creating a stratified current along the floor. In the current design, the supplied air enters the room directly, leading to potential problems such as high draught rates.

Addressing this issue is an essential step in improving the design of Notech so that its potential use in school is enhanced. Therefore this paper focuses on understanding the current performance of the panel in regards to air activity in the filter and draught rates. Furthermore, these results and observations are used to propose solutions for optimization.

## 1.2 State of art

This chapter summarizes the latest findings on Notech panel in connection to its performance and design acquired from the Technological Institute and WindowMaster. Moreover, discusses the current use of draught models in the building industry.

### 1.2.1 Notech natural ventilation panel

Notech is an architectural indoor climate solution for new constructions and renovations based on natural ventilation and natural materials. The ventilation is provided through the façade panel where moisture and noise absorbing eelgrass serves as a filter and insulation between the outdoors and the occupied space. This natural ventilation solution can provide an efficient strategy for heavily polluted spaces, such as classrooms, while insulating from outside noise and allowing secure venting in unoccupied hours, which are some of the main challenges with traditional venting through windows. [12]



However, the Notech solution has its own challenges, such as high pressure loss caused by the filter, which hinders the ability to ensure sufficient airflow into a room. This had been addressed by the Technological Institute and their study led to removal of the textile fabric (inner filter) in the latest version of the panel to minimize the pressure loss as it was also found not necessary for the performance of the panel. In cases where the air exchange is too low, a controlled axial (propeller fan) can help the Notech panel to achieve the needed air exchange. The controlled axial will have a low-pressure performance, and thereby have a lower electricity consumption than a ventilation system consisting of ducts and two fans – intake and extraction.

For the draught rate, it was found that it exceeds the acceptable 20% under different conditions: air intake (e.g. 75 l/s and 50 l/s) and temperature difference between outside and inside (e.g. 16.0 dT and 12.3 dT), where the heat source was floor heating. In addition to this, an investigation with electric radiator as heat source, was also carried out. The conditions under the experiment was air intake of 35 l/s and temperature difference of 18.1 dT, the power of the radiator was 1300 W. It showed that the radiator improved the problem, since it reduced the draught rate in the occupied zone to below 20%.[11] [12]

### Construction of the current model of the Notech panel

The Notech panel consists of two parts – active and passive section. The active section where the air is entering and penetrating through the panel is situated at the top of the construction and has following dimensions: (HxWxD) 1.12 x 0.598 x 0.115 m (app. fig. A.32). The opening area is defined as a sum of area on the bottom, side and top of the opening. The measured opening area at 100% window opening is 0.18 m<sup>2</sup> which corresponds to 13.5°. Opening area at 33% window opening is 0.14 m<sup>2</sup> which corresponds to 4.5°. It consists of a side hinged opening and an eelgrass filter (fig. 1.1). The passive part does not have a ventilation function and serves as a storage for associated equipment. The element is covered with a wooden cladding on the inner side and a rain screen on the outside.

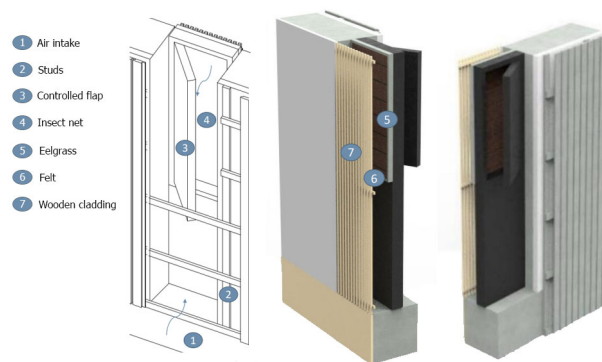


Figure 1.1: Notech panel design drawing [12] [1]

### 1.2.2 Draught models

The draught rate (DR) provides a way to evaluate the potential percentage of people dissatisfied due to draught. There are different draught rate models, which are appropriated for different areas of the human body. The draught rate model that is used predominantly in the current Danish building regulations, is designed to predict draught rate at the neck area. However, in today's context, with the prevalence of alternative air distribution systems and the emergence of new thermally stratified systems, it fails to address another significant area – ankle level.

For this reason, different draught rate models are investigated in this research paper. This is done to analyze and assess the risk of draught from the natural ventilation system, in relation to different draught assessment methods, which is appropriated for different areas of body.

The three draught models evaluated in relation to estimating the risk of draught at ankle level from a natural ventilation system are; Fanger's model used predominantly in danish building practice, Fanger's model corrected to ankle level and the draught rate model for ankle from ASHRAE 55:2021. [15] [10]

#### Draught model - Fanger's

Fanger's draught rate model from 1988 is used in thermal comfort standards ISO 7730:2005 and EN 16798-1:2019. This model is made to predict the draught rate at the neck level. It applies to people with a mainly sedentary activity and close to neutral thermal sensation for the whole body.

The elements which influence the draught rate in this model are local air temperature, the mean air velocity and local turbulence intensity.

The draught rate is calculated according to the equation 1.1:

$$DR = (34 - t_{a,l}) \cdot (\bar{v}_{a,l} - 0.05)^{0.62} \cdot (0.37 \cdot \bar{v}_{a,l} \cdot T_u + 3.14) \quad (1.1)$$

Where,

DR is draught rate, %

$t_{a,l}$  is local air temperature, °C 20-26°C

$\bar{v}_{a,l}$  is local mean air velocity, m/s, <0.5 m/s

$T_u$  is local turbulence intensity, %, 10-60%

The model is not well suited for predicting draught rate at the arm or feet level, as it is expected that it could overestimate the predicted draught rate at these areas. [2] [4]

### Draught rate - Fanger's corrected to ankle level

A comparison between the draught rate for neck and its expected overestimation of draught rate at arm and feet level was conducted by Fanger. It compared the people dissatisfied with draught according to the draught rate model for neck level, with a measured number of dissatisfied due to draught rate at arms and feet level. The result from this comparison is seen in fig. 1.2. [8]

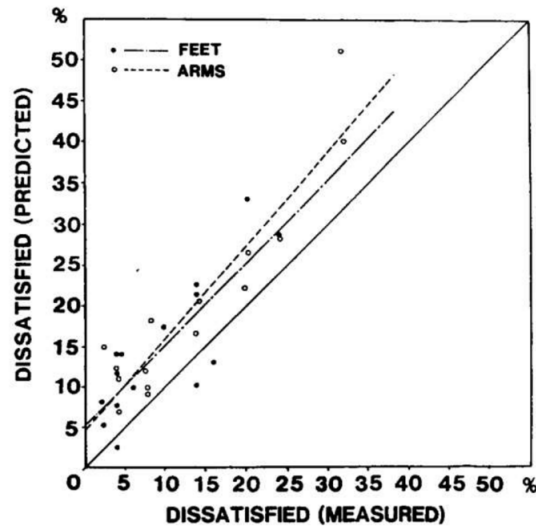


**Figure 1.2:** The comparison between the predicted and measured percentages of draught risk at arms and feet level [8]

This shows that there are a close to linear correlation between the draught rate model for neck level and the taken measurement for dissatisfied at arm and feet level. It is therefore possible to calculate from this, what the expected draught rate should be at the neck, arm and feet level.

Based on fig. 1.2, Fanger's draught rate model for neck adjusted to feet level, can be achieved by implementing a correlation coefficient of 0.82. The corrected draught rate model for feet level can be seen in equation 1.2:

$$DR = ((34 - t_{a,l}) \cdot (\bar{v}_{a,l} - 0.05)^{0.62} \cdot (0.37 \cdot \bar{v}_{a,l} \cdot T_u + 3.14)) \cdot 0.82 \quad (1.2)$$

### Draught rate - ASHRAE 55: 2021

Another draught rate model can be found in the thermal comfort standard ASHRAE 55:2021 'Thermal Environmental Conditions for Human Occupancy'. This draught model

differs from Fanger's draught model, as it is made to predict percentage of people dissatisfied due to draught at the ankle level. The draught rate is calculated according to the equation 1.3:

$$PPD_{AD} = \frac{\exp(-2.58 + 3.05 \cdot V_{ankle} - 10.6 \cdot TS)}{1 + \exp(-2.58 + 3.05 \cdot V_{ankle} - 1.06 \cdot TS)} \quad (1.3)$$

Where,

$PPD_{AD}$  is predicted percentage of dissatisfied with ankle draft, %

$TS$  is whole body thermal sensation; equal to PMV calculated using the input air temperature and and speed averaged over two heights (for seated person 0.6 m and 1.1 m)

$V_{ankle}$  is air speed at 0.1 m above floor level, m/s

The maximum allowed air speed at 0.1 m above the floor can be calculated with equation 1.4:

$$V_{ankle} < 0.35 \cdot TS \cdot 0.39 \quad (1.4)$$

For the calculation of the ASHRAE draught model, an online CBE Thermal Comfort Tool is implemented. The tool for ankle draught uses air temperature, mean radiant temperature, air speed, ankle level air speed, humidity, metabolic rate and clothing level to calculate the draught rate at ankle level. The air temperature and air speed are average temperatures over two heights (0.6 m and 1.1 m for seated person). Air speed on the upper body should not exceed 0.2 m/s when using this ankle draught model, as a higher air speed than 0.2 m/s should refer to the elevated air speed model instead. Metabolic rate of 1.2 met is set for a sedentary activity. Clothing level is assumed for a seated person in school environment. The model is made for a lightly clothed person – clothing insulation between 0.5 and 0.7 clo. With the use of equation 1.3, it is therefore recommended to keep the clothing under 0.7 clo, but it is acceptable to implement the use of higher clothing levels. The higher insulation level is only making the results more conservative, because the increase in clothing insulation is making people less thermally sensitive. However, this paper uses the online tool - CBE, where the upper clothing limit is 0.7 clo. [10]

### 1.3 Problem formulation

In order to investigate the issue of draught and suggest possible improvements, this report focuses on testing and understanding the current design of the panel regarding airflow through the eelgrass filter and shortly after entering the room. Furthermore, the panel is tested for draught rates under variable pre-determined conditions. Lastly, new design solutions are proposed and tested with the aim to extend the limits of the panel performance regarding draught rates. The research will be carried out answering following questions:

- 1. What is the current performance of the Notech panel regarding the inlet opening activity?**
- 2. What are the current draught rate limits and how does the position of the venting opening influence the draught rate?**
- 3. How does the choice of draught model impact the interpretation of results?**
- 4. What solutions could be implemented with Notech prototype to extend the limits of the panel regarding the draught rate?**

The defined questions are addressed through a systematic conduction of experiments on the Notech prototype, provided by WindowMaster, within the laboratory settings.

### **1.3.1 Limitations**

In this section, various limitations concerning the project are stated to provide context to the employed methodology and interpretation of the results. The scope of the project is inherently shaped by the availability of the laboratory and laboratory equipment provided by the Aalborg University. As a result, the investigation of the Notech panel is carried out in the period of 30.10 - 15.12. and focuses only on draught issue, excluding exploration of other elements related to the thermal comfort.

The limitation extends to the availability of 12 working anemometers, with only 11 capable of measuring temperature accurately. As a result, the placement of them is tactically altered between steps and stages during experiments. Moreover, strategic choices are made to restrict the amount of performed measurements, such as stopping measurements once all models indicate draught rate over 20%. Additionally, only one set of measurements per case is performed in the centre of the panel when investigating the current performance of the unit. During the measurements, the anemometers for CBE are placed solely on the border of the measuring zone. Some measurements are limited based on predicted performance of the solutions.

The choice of other equipment is dependent on its availability in the laboratory. To measure the operative temperature, an IC meter is installed in each room. However, it is noteworthy that IC-meters display temperature data every 5 minutes, restricting precision of monitoring the temperature throughout the experiments. Consequently, impeding the timely achievement of the desired temperature differences. Moreover, the cooling and heating settings require manual manipulation. The heaters in the hot room have only two power settings, 1000 W and 2000 W. Furthermore, the passive section of the Notech panel was installed next to the unit, instead of underneath it, therefore placement of radiator in it is not possible for investigation.

The laboratory setup is restricted by both the construction materials used and objects already present in the rooms. During the measurements it is observed that the door separating the cold and hot room have to some degree influence on the results, due to high transmission losses and leakage (app. fig. C.33). Furthermore, as the test rooms accommodate various experiments simultaneously, additional equipment and furniture are stationed in these spaces. This is thought to pose a potential obstacle to the airflow, resulting in an increase in air velocity at the anemometers located furthest within the room (at the border of the measurement zone).

It is found that calculating the draught rate with Fanger's formula (ISO 7730) is not possible if the values for air velocity are smaller than 0.05 m/s. In these cases, the draught rate is considered to be 0.

## Chapter 2

# Methods

The following chapter outlines the systematic approach employed for conducting experiments with the Notech panel to answer the research questions.

### 2.1 Laboratory setup

The experiments are performed in a laboratory setting within a designated test room - hot chamber, which is intended as mock-up of a 1/4 of a classroom. The hot chamber is adjacent to cold room that is designed to simulate outdoor temperature conditions. Both rooms are insulated and used to create desired temperature differences, under which the measurements are performed. The plan drawing of the setup can be seen on fig. 2.1.

The hot room dimensions are (LxWxH) 4.2 x 3.6 x 2.5 m and the heat is supplied by two electric radiators outside of the examined area. The examined area (measurement zone) presents the area with the highest risk of draught - 1.5 m from the panel. The Notech panel is mounted in the partition wall (insulated with 0.15 m polystyrene board) between the cold and hot room, according to instructions from the developer.

The air is supplied from the outdoors to the cold room, where it is cooled down by the cooler to a desired extent. The cold air then penetrates the Notech panel and enters the hot room. The amount of airflow through the panel is regulated by an exhaust fan in the hot room. The operative temperature in each room is measured by IC-meter, located in the middle of the room at height of 1.1 m. To prevent high vertical temperature gradient in the hot room, a fan is utilized to mix the air, and is turned off right before performance of the measurements to avoid its influence on the flow.

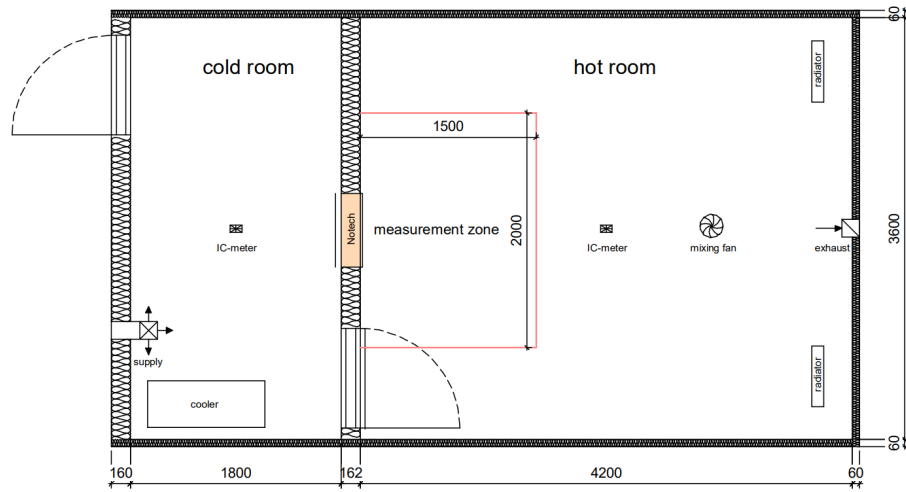


Figure 2.1: Plan of the laboratory rooms and setup, dimensions in mm

## 2.2 Measurements procedure and conditions

The conditions defined and changed during the experiments are the panel height position, opening of the inlet, flow rate through the panel and temperature difference ( $dT$ ) between hot and cold room. The detailed explanation for reasoning behind the chosen conditions can be seen in the app. ch. A.1.

### Panel position heights

The panel's height is determined in two positions: first, at the top (starting at 1 m above the floor), and second, at the bottom (floor level). See pictures in app. fig. A.1.

### Opening of the inlet

It is decided to work with the panel fully open (100% opening, corresponding to  $13.5^\circ$ ) and with a fraction of the panel open (33% opening, corresponding to  $4.5^\circ$ ).

### Temperature differences ( $dT$ )

The internal operative temperature used in the hot room is  $22^\circ\text{C}$ , based on the Danish standard ISO 7730 category B. The outdoor temperatures chosen for the winter period are  $-5^\circ\text{C}$ ,  $0^\circ\text{C}$  and  $10^\circ\text{C}$ , resulting in temperature differences of:

- $27^\circ\text{C}$
- $22^\circ\text{C}$
- $12^\circ\text{C}$



### Flow rate

The flow rates are designed based on the assumed number of students in the classroom and number of panels installed there, as well as the requirements for the CO<sub>2</sub>, resulting in:

- 71 l/s
- 47 l/s
- 35 l/s

Panel height position	Temperature differences	Flow rate	Opening
	$\Delta T$	l/s	%
lower - floor level	$27^{\circ}\text{C} \pm 0.5$	71	100
			33
		47	100
			33
		35	100
			33
	$22^{\circ}\text{C} \pm 0.5$	71	100
			33
		47	100
			33
		35	100
			33
	$12^{\circ}\text{C} \pm 0.5$	71	100
			33
		47	100
			33
		35	100
			33
upper	$27^{\circ}\text{C} \pm 0.5$	71	100
			33
		47	100
			33
		35	100
			33
	$22^{\circ}\text{C} \pm 0.5$	71	100
			33
		47	100
			33
		35	100
			33
	$12^{\circ}\text{C} \pm 0.5$	71	100
			33
		47	100
			33
		35	100
			33

Figure 2.2: Overview of all combinations of conditions

#### 2.2.1 Stage 1

In the first stage of the measurements, the goal is to investigate the behavior of airflow through the panel and to determine the limit, at which the draught rate exceeds 20%, according to the three models described in subch. 1.2.2.

In the first step, the airflow through the opening is examined using a thermal camera to detect which part of the eelgrass filter is active. The stage 1 step 1 is performed under all the presented conditions. For this experiment, the location of the panel is not relevant.

In the second step, the draught rate is evaluated under different conditions by utilizing the measured data from the anemometers (air velocity, temperature and turbulence intensity) at the border of the measurement zone. The placement of the measuring points for 16 channel Dantec 54N10 hot sphere anemometers can be seen on fig. 2.3 and 2.4. The anemometers at the horizontal pole are situated at the standard ankle height - 0.1 m, every 0.3 m. The spacing of the anemometers on vertical pole differs depending on the panel

height position. Additional vertical pole at the border of the measuring zone is added for the ASHRAE draught model. Furthermore, mean radiant temperature is measured once per each condition for the CBE tool (app. ch. C.2.1).

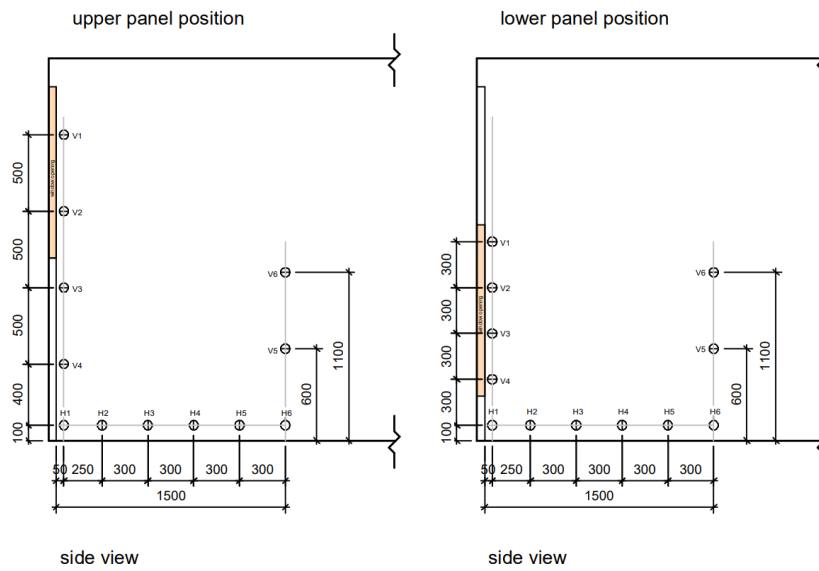


**Figure 2.3:** Stage 1 Step 2 - side view of measuring points setup, dimensions in mm

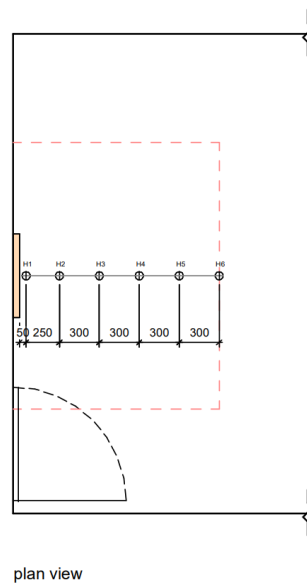


**Figure 2.4:** Stage 1 Step 2 - plan view measuring points setup, dimensions in mm

The measurements are conducted starting from the lowest temperature difference and the smallest airflow, progressing to higher values. Measurements are terminated once the draught rate of 20% is exceeded in all three models, with the exception of 27 dT (read the explanation in app. ch. C.2.4).

### 2.2.2 Stage 2

After stage 1, the results are analyzed and solutions for improvement are suggested. In stage 2, the solutions tested for draught are:

- **Inlet design**

Different sides of the intake through cover are taped (bottom, bottom and right side, bottom and both sides), to force the supplied air to be distributed more evenly.

- **Heater**

Heater positions and amount of supplied power are tested to examine their influence on the draught rate. The positions are: in front of the panel at both floor level and directly underneath the inlet (app. fig. A.7). The supplied power is corresponding to either 100% or 50% of the calculated ventilation loss.

- **Shelf systems**

Different types of shelf systems are evaluated: solid shelves, solid shelves with edges and perforated shelves with edges. Moreover, the influence of the number of shelves is also analysed (cases with 1 and 5). The shelves are installed to disrupt the boundary layer flow along the vertical surface, enforcing mixing of the cold supplied air with the air in the room and to decrease the air velocity.

After the initial testing of the proposed solutions and analysing the results, the two different shelf system designs are combined with a heater. Firstly, the original design of five shelves and later only one middle shelf is kept.

The anemometers for stage 2 are placed on two horizontal poles, at 0.1 m height, around every 0.4 m (fig. 2.5). The two poles are moved during the measurements, in order to create a grid of the measuring zone, enabling more comprehensive analysis of the influence of the proposed solutions on the draught rate.

The performed combinations of measurements and their sequence are chosen individually for each solution based on the obtained results from previous stage (fig. 2.6).

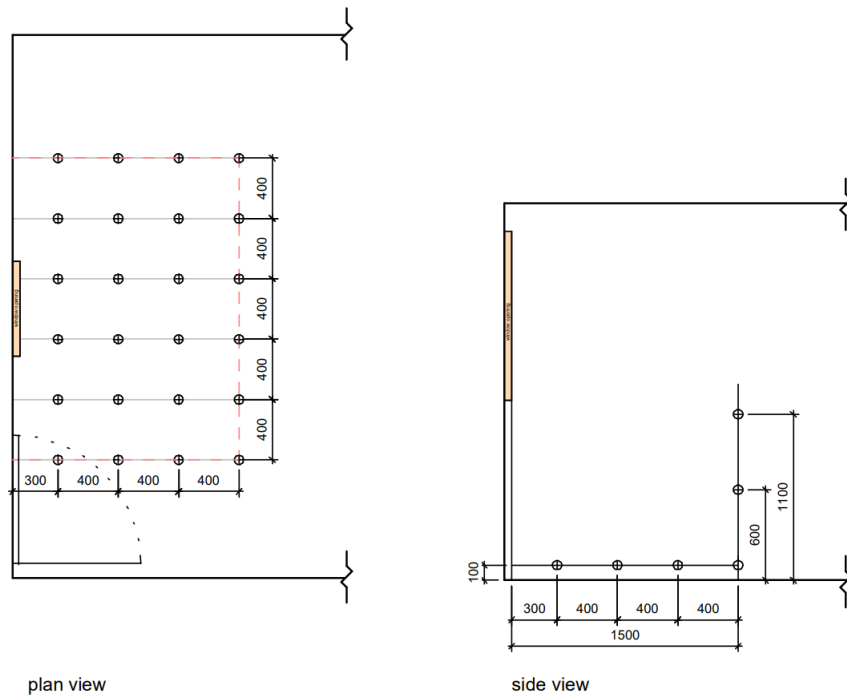


Figure 2.5: Stage 2 measuring points setup

order	$\Delta T$	1/s	opening	power	solution	Method
1.	12	35	0%	-	inlet bottom sealed	thermographic camera
2.	12	35	33%	-	inlet bottom sealed	
3.	12	35	100%	-	inlet bottom sealed	
4.	12	47	33%	-	inlet bottom sealed	
5.	12	35	33%	-	inlet right side + bottom sealed	
6.	12	47	33%	-	inlet right side + bottom sealed	
7.	12	35	33%	-	inlet both sides + bottom sealed	
8.	12	47	33%	-	inlet both sides + bottom sealed	
1.	12	35	33%	-	not sealed inlet	anemometers
2.	12	35	33%	-	inlet sealed on the bottom	
1.	27	71	100%	2000W	heater on floor	
2.	27	71	100%	1000W	heater on floor	
3.	27	71	33%	1000W	heater on floor	
4.	27	71	100%	1000W	heater under inlet	
5.	27	47	100%	1000W	heater on floor	
1.	22	47	33%	-	solid shelves	
2.	22	47	100%	-	solid shelves	
3.	22	71	100%	-	solid shelves	
4.	22	47	33%	-	solid shelves with edge	
5.	22	47	100%	-	solid shelves with edge	
6.	22	71	33%	-	solid shelves with edge	
7.	22	47	33%	-	perforated shelves with edge	
8.	22	47	100%	-	perforated shelves with edge	
9.	22	71	100%	-	perforated shelves with edge	
10.	27	71	100%	1000W	perforated shelves with edge + heater	
11.	22	71	100%	-	single perforated shelf with edge	
12.	22	47	33%	-	single perforated shelf with edge	
13.	27	71	100%	1000W	single perforated shelf with edge + heater	

Figure 2.6: Overview of conducted measurements for stage 2

## Chapter 3

# Findings

This chapter summarizes all the main findings from the experiments performed in the AAU laboratory in the period of 30.10 - 15.12.2023. It includes a brief description of the methods and goals, while referring the rest of the findings and data to appendix. It is divided into 2 stages. The first one focuses on understanding the current design and the second one proposes solutions for optimization based on findings from stage 1 and on-going analysis of results from stage 2.

### 3.1 Stage 1

Stage 1 of the project focuses on measuring and understanding of the current design of the panel. The stage is divided into two steps. In the first step, thermographic pictures are taken under all the predetermined conditions (fig. 2.2). The aim of this step is to determine the parts of eelgrass filter that are active under different conditions. This knowledge gives an understanding of the current design to be later used in solution proposal. The aim of the second step is to determine the limits of the panel in regards to draught. The Notech is exposed to different conditions and tested for draught rate until it reaches unacceptable levels in all three DR models. In this step, the position of the panel is altered between upper and lower (fig. 2.3) to see a potential of this variation for use in the next stage.

#### 3.1.1 Step 1 - thermography

In the first step, the Notech panel is subjected to different conditions under which thermographic pictures are taken and analysed. The variable conditions are temperature differences (12, 22, 27°C), airflows (35, 47, 71 l/s) and opening of the inlet (33, 100%). For each section of the panel (fig. 3.1), the average temperature is calculated based on data from 3 points within that section. A dimensionless temperature is defined by outdoor and indoor temperature (outdoor temperature = 0, indoor temperature = 1). Then the temperature gradient between each section is determined and the values are normalized.

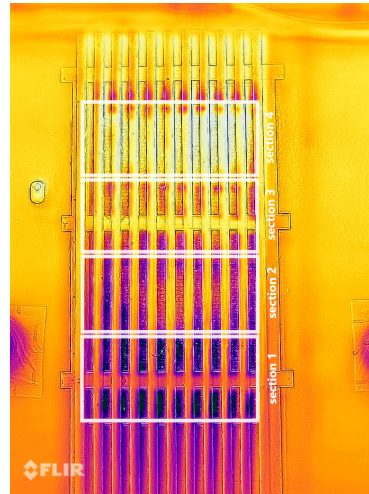


**Figure 3.1:** Thermographic picture of the Notech panel with marked sections

The analysis shows that similar trends are present in all the cases, as shown on fig. 3.2. The instances where temperature of the Notech panel is higher than the surrounding temperature in the hot room ( $>1$ ) should be disregarded, as they are caused by the vertical temperature gradient that was present in the room during the measurements. Based on the graph, it seems that the temperature differences do not have high influence on the air distribution (fig. 3.3), unlike the airflow and the opening of the inlet.

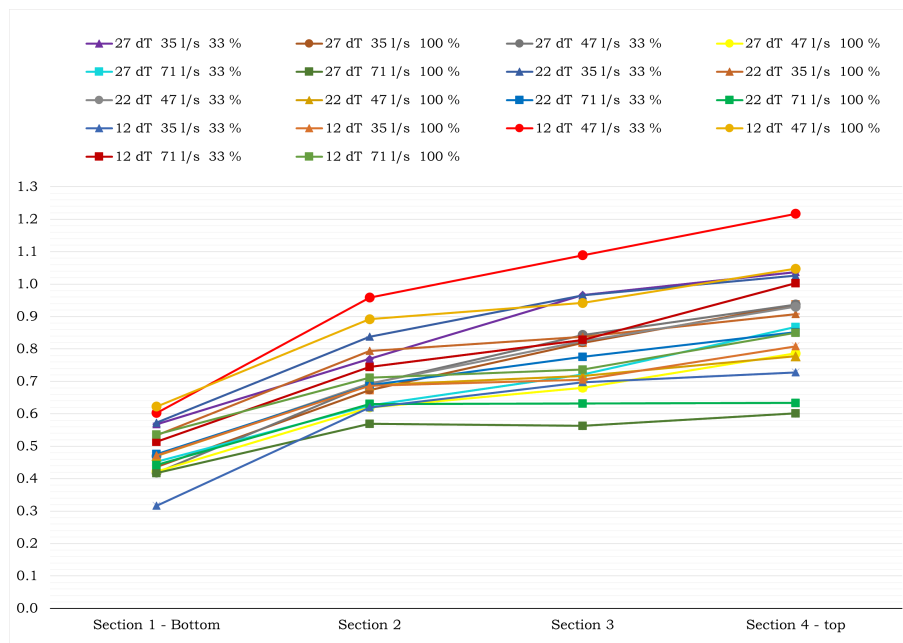


**Figure 3.2:** Overview of the temperature difference across the panel under different conditions

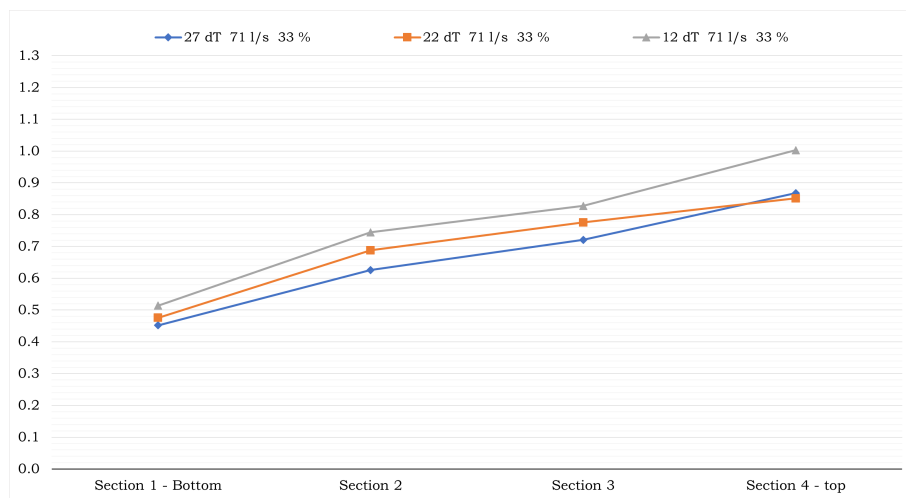


**Figure 3.3:** Comparison of temperature gradient under the same airflow (71 l/s) and inlet opening (33%)

Based on the thermography (fig. 3.4 - 3.6, also app. ch. C.1) it can be seen that the higher the airflow and inlet opening, the more area of the panel is penetrated by the supplied air and the more even the air distribution is throughout the unit. The whole panel is the most active at 71 l/s and 100% inlet opening, while at lower airflows (35 and 47 l/s) and 33% opening, mostly the bottom 2 sections are active, as indicated by the lower temperature. These results give an understanding of the air movement through the panel which can be used in the future for design changes.

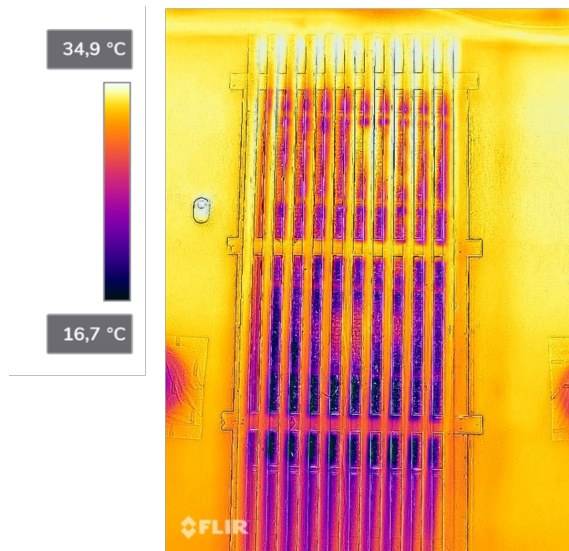


**Figure 3.4:** 27 dT, 71 l/s, 33%

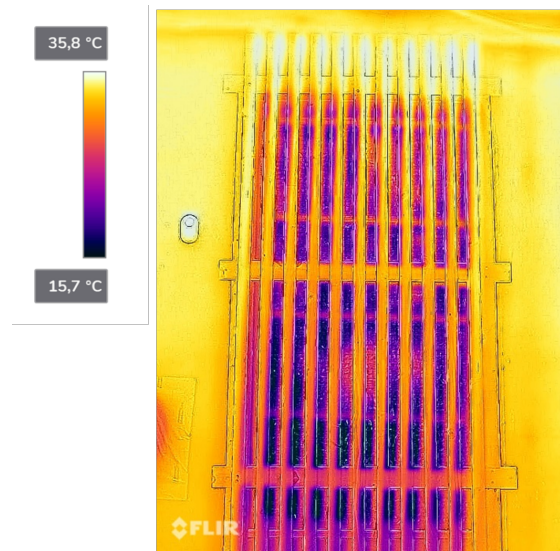


**Figure 3.5:** 27 dT, 71 l/s, 100%

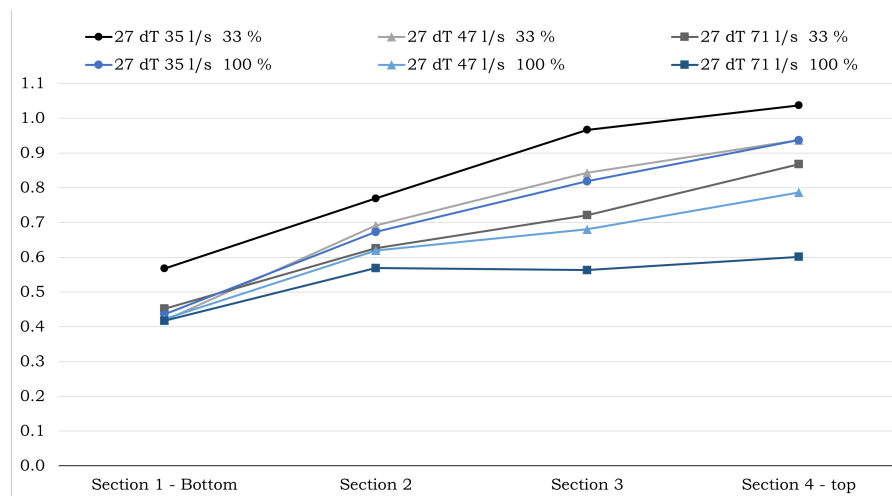


Figure 3.6: Temperature difference across the panel at 27 dT

### 3.1.2 Step 2 - draught rate

In the upcoming section, analysis of the velocity and temperature development, as well as the evaluation of the draught rates are presented for various conditions, which are mentioned in methodology ch. 2.2. The graphs for velocity and air temperature display results from the panel up to a distance of 1.5 m from the wall, whereas for the draught rate results for measuring points located at the border (1.5 m) are considered. The positions of the anemometers can be seen in fig. 2.3.

#### Velocity development

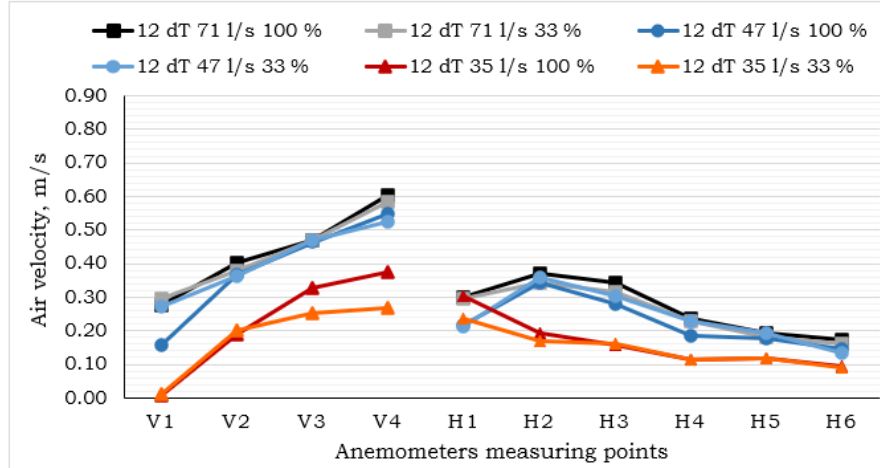
##### Velocity for upper panel height position

Fig. 3.7 shows the air velocity development patterns under a constant temperature difference of 12°C, with different airflows and inlet openings. The air falling along the wall increases in speed, due to gravity force, until it reaches the floor level, where its kinetic energy transforms to pressure, thus the velocity decreases. After that, the pressure is transformed back into kinetic energy again, which can be seen on the velocity increase at the horizontal measurement points. The distance at which this happens depends on the volume flow. In this instance, the increases can be seen transpiring before H1 or from H1 to H2.

The air velocity development patterns is similar for the cases with a temperature differences of 22°C and 27°C (app. fig. C.10-C.11). The cases for 27°C temperature difference and airflow of 35 l/s (app. fig. C.11), does however contain an abnormal behavior in the air velocity development between H5 and H6. The air velocity starts to increase from H5 to H6, which is the opposite of what is expected to be seen, as velocity should be slowed



down by entrainment. It is not known for certain what is causing this increase, but it could be caused by an obstacle deeper in the room posing a resistance for the flow, thus resulting in higher velocity.



**Figure 3.7:** Velocity development at 12 dT (upper panel height position)

### Velocity for lower panel height position

Fig. 3.8 shows the air velocity development patterns under a constant temperature difference of 12°C, with different airflows and inlet openings. The pattern reaches the highest horizontal values at the second anemometer (H2). These velocities are then decreasing at a very moderate pace, almost kept at constant values throughout the near zone, which is thought to be occurring due to air being directly supplied at this height. The temperature difference between the current along the floor and the room might be creating a gravity current. This would result in smaller entrainment, causing the moderate decrease.

The air velocity development patterns is behaving similarly for the cases with a temperature differences of 22°C and 27°C, (app. fig. C.12-C.13.) Both have the moderate decreasing pace for the air velocity and highest value at the second anemometer. In the 22 dT case, the H1 and H2 are almost identical to each other.

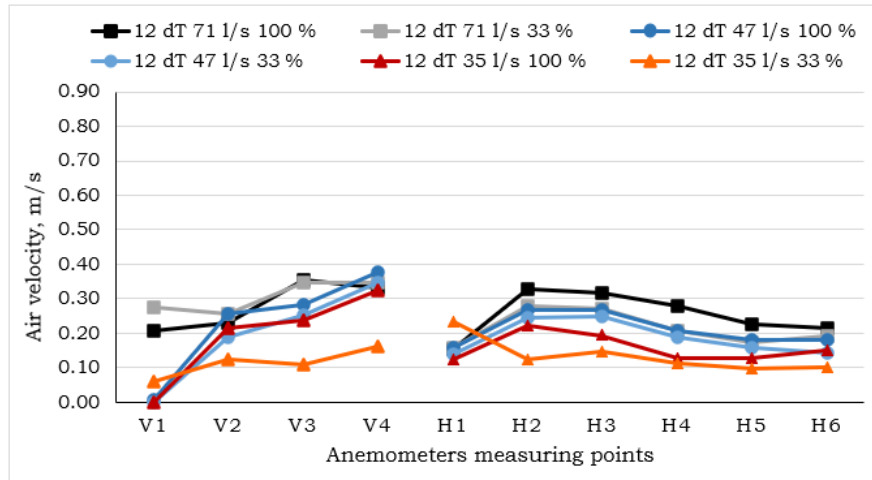


Figure 3.8: Velocity development at 12 dT (lower panel height position)

### Panel height position comparison

Fig. 3.9 shows the comparison of velocity development for upper and lower position, under the conditions 27 dT, 35 l/s, 33 and 100% opening. The velocity gain at the upper position caused by gravity forces is close to the amount of energy it loses in the transformation of kinetic energy to pressure. The air velocities for the lower and upper position are close to each other when they hit the first horizontal measurement point (H1). This results, in combination with the moderate decrease in air velocity at the lower position, that the lower position has a higher air velocity at the last measurement point (H6). Similar trend is seen under other conditions (app. fig. C.16-C.19).

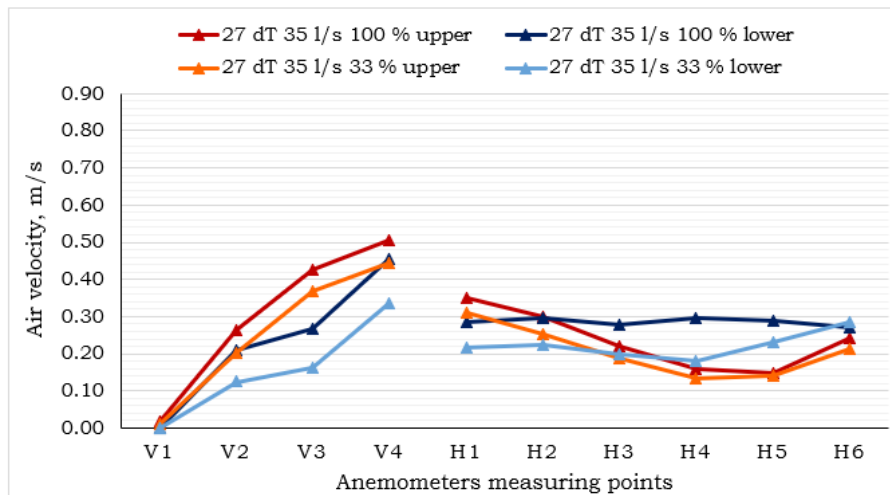


Figure 3.9: Comparison of velocity development at different panel height positions at 27 dT, 35 l/s

### Air temperature development

The desired outdoor temperatures (-5, 0, 10°C) are reached by creating a temperature difference between the cold and hot room. The cold room is cooled down to approximately 6°C and the difference is adjusted with heating in the hot room. The starting temperature in the hot room is considered 22°C in all setups, regardless of the actual room temperature, as long as the desired temperature difference is kept. For measurements to be comparable and to compensate for inaccuracies, the measured air temperatures are corrected according to the temperature at the chest level (1.1 m from the floor) and at the border of the near zone (1.5 m from the panel). This measured air temperature - V6 (fig. 2.3), is corrected with a value to reach 22°C. The rest of the air temperature measurements in the same experimental setup are corrected with the same value.

In all of the cases (app. ch. C.2.3) the same pattern emerges - the air temperature drops along the vertical surface and starts to increase with the horizontal distance due to entrainment until it reaches the room temperature.

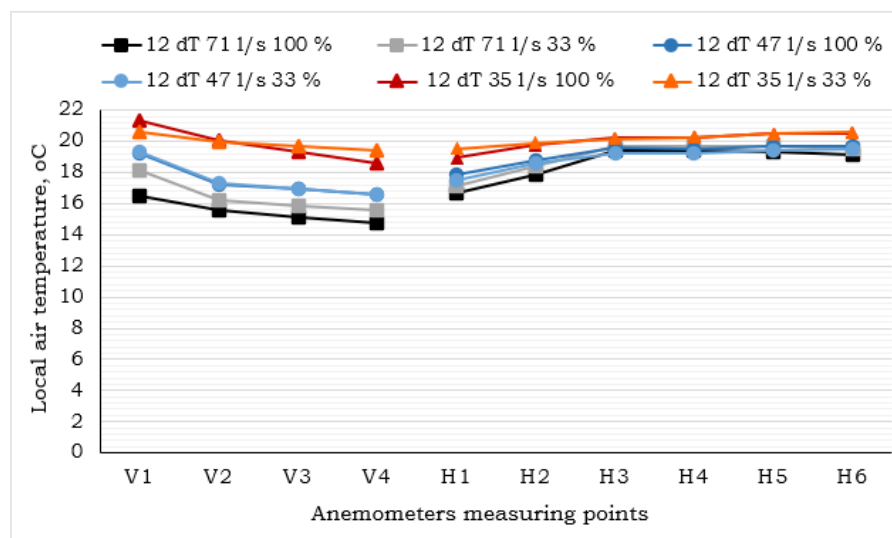


Figure 3.10: Temperature development at 12 dT (upper panel height position)

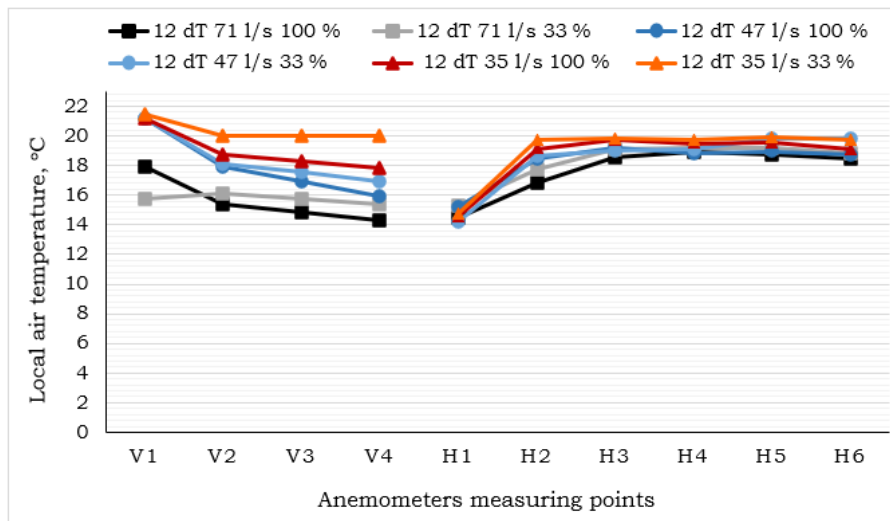


Figure 3.11: Temperature development at 12 dT (lower panel height position)

### Draught rate and model comparison

This section compares draught rates reached at different flow rates, inlet openings, temperature differences and panel height positions using CBE draught comfort tool, Fanger's draught model from ISO 7730 and Fanger's draught model corrected for ankle height. The models are used to determine limitations of the panel at different setups. The evaluation point for the draught rate is positioned in front of the center of the panel, at the border of the measuring zone - 1.5 m (H6) from the panel (fig. 2.3 and 2.4). However, due to the abnormal behaviour of the velocity (subch. 3.1.2), some of the values used for calculating DR were changed to a lowest measured velocity from position H4, H5 or H6 to account for the obstacle (further explanation can be seen in app. ch. C.2.4) For CBE model, the air and mean radiant temperature were taken on site (and corrected for 22°C, app. ch. C.2.1).

### Draught rates for the upper and lower panel height position

The figures 3.12-3.14 show performance of the panel for both upper and lower panel height position using all three models.

CBE model (fig. 3.12) shows acceptable draught rates for all the 12 dT setups at the upper position of the panel. At 22 dT, the rates start to be unacceptable with higher flows, with an exception of 71 l/s 33% opening. For the lower position of the panel the draught rate becomes problematic already at the 12 dT for the highest flow and persists across various temperature differences.

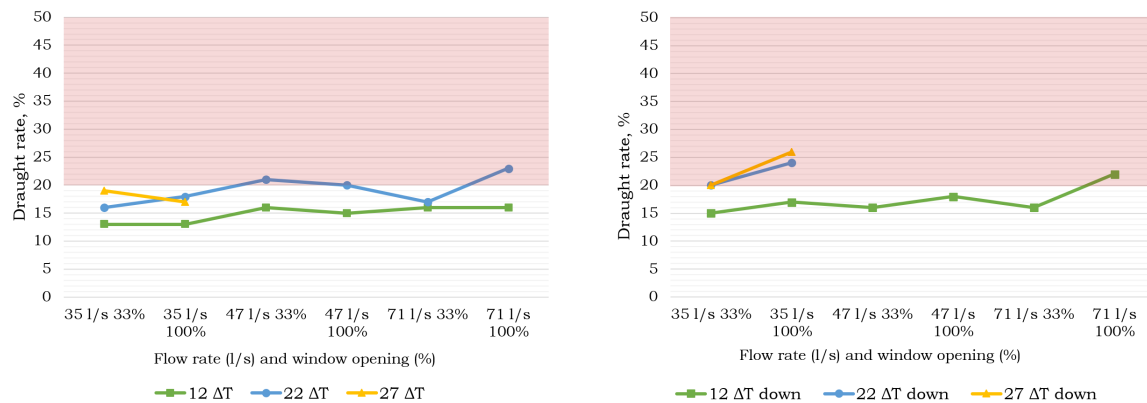


**Figure 3.12:** Results for CBE ankle draught model for all cases, for both upper (left) and lower (right) panel height position. Results exceeding draught limit (20%) are marked with red area

Fanger's model corrected for ankle (fig. 3.13), similarly to the CBE, demonstrates acceptable draught rates at 12 dT for the upper panel position, while exceeding the limit at highest flow for the lower position. For the upper panel height position it reaches its limit at 22 dT 47 l/s and for the lower position at 22 dT 35 l/s.

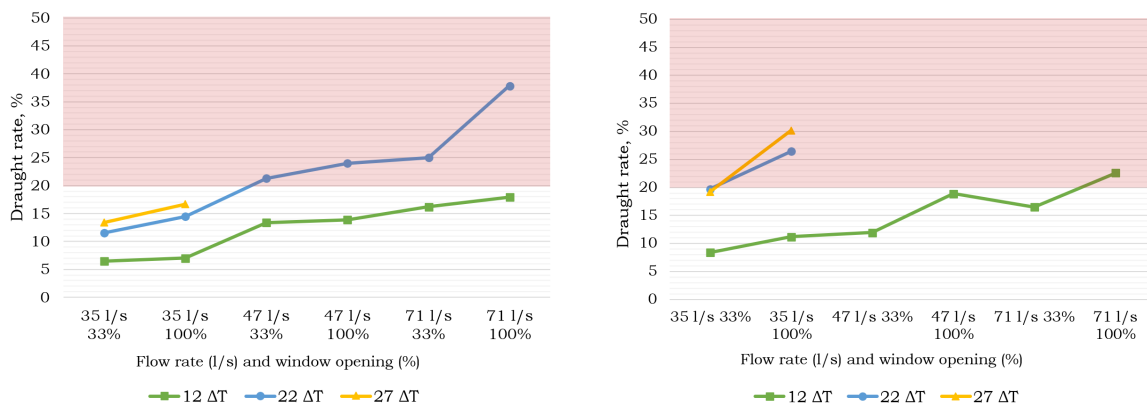


**Figure 3.13:** Results for Fanger corrected for ankle draught model for all cases, for both upper (left) and lower (right) panel height position. Results exceeding draught limit (20%) are marked with red area

Fanger's model for neck (fig. 3.14) reaches unacceptable draught rate at 12 dT not only for the lower panel height position, but also for the upper position. Overall, it reaches the highest value of all of them - over 45%.

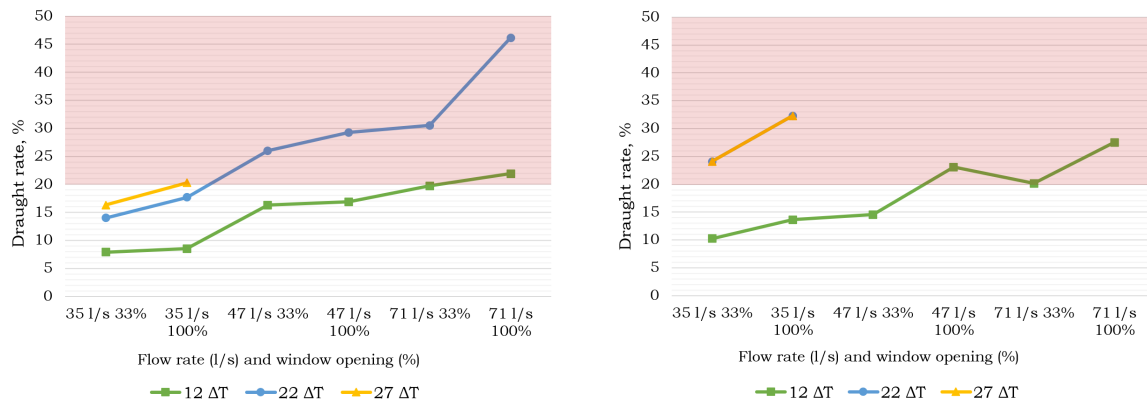


**Figure 3.14:** Results for Fanger (ISO 7730) draught model for all cases, for both upper (left) and lower (right) panel height position. Results exceeding draught limit (20%) are marked with red area

From the experiments and applied methods, it is clear that the Fanger's model for neck is the strictest of all of them. The other two models, made for ankle level, show less critical values. It cannot be said which model is the least strict throughout all the experiments as it depends on the specific conditions.

At the beginning of the measurements, the hypothesis was that lowering the panel position would influence positively the draught rates due to the fact that lowering the panel position prevents cold air from descending as far, hence minimizing increase in the velocity. However, the experiments contradicted this hypothesis. Through repeated measurements involving varying temperature differences, air flows, and opening angles, it became evident that lowering the panel height position does not improve the draught issue. Consequently, the following research is conducted only for the upper panel height position.

### Draught model comparison

The figures 3.15 and 3.16 compare 3 different draught models and demonstrate what effect the use of draught model has on the resulting percentage of dissatisfied. Fanger's draught model from ISO 7730, shows the highest rates of draught for the majority of the experiments. This model is designed to predict dissatisfaction with draught at neck level. The results from Fanger corrected for ankles are a direct correlation of the first Fanger draught model results and thus show lower dissatisfaction rate at a steady pattern. The CBE model results vary significantly with the different temperature inputs, as it takes into consideration the predicted mean vote. Therefore, even at small  $dT$  and airflows, it still reaches relatively high values (due to low air temperatures). It is important to mention that the CBE model is limited to 0.7 clo which is not necessarily typical winter clothing. Therefore, it can be assumed that with higher clothing levels, the PPD would decrease.

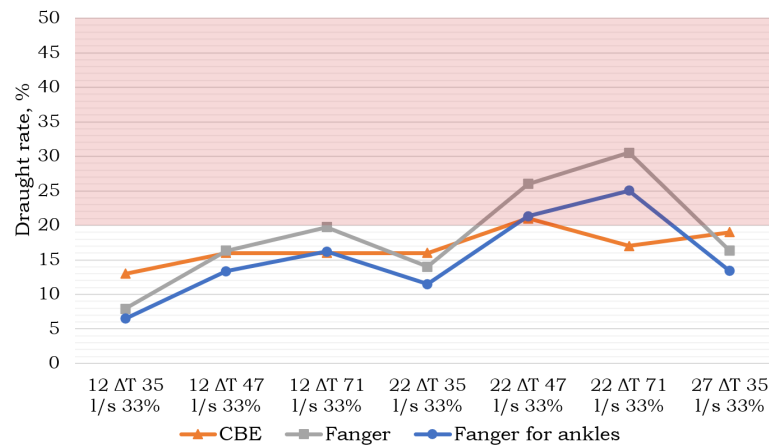


**Figure 3.15:** Draught model comparison for upper panel height position, 33% opening of the inlet

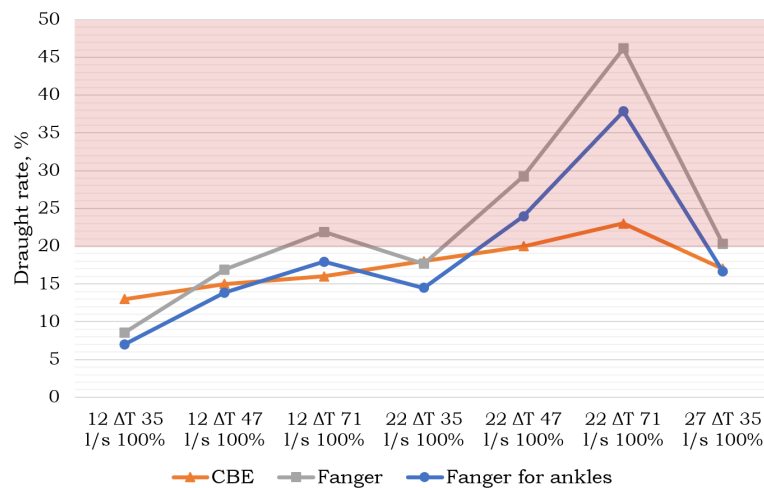


**Figure 3.16:** Draught model comparison for upper panel height position, 100% opening of the inlet

### Summary

In summary, the research outcome recommends using Fanger's model corrected for ankle for further analysis. This preference arises from the observed limitations of the alternative models in determining draught at ankle level during winter condition. The Fanger for neck overestimates the results as it is meant for a sensitive and more exposed body part, and the CBE does not consider typical winter clothing level, which is higher than 0.7 clo. Furthermore, it was found that lowering a position of the panel does not improve the draught issue, therefore the research continues with the original panel height.

It is corroborated that the use of Notech panel indeed results in issues with draught under specific conditions. The problem becomes apparent at combinations of low outdoor temperatures (0 and -5°C) and higher airflows (47 and 71 l/s). While higher airflows ensure

good atmospheric comfort, they come at the expense of thermal discomfort. Conversely, lower airflows do not seem to cause draught issues, but they fail to provide sufficient air supply for optimal atmospheric comfort. This means that under tested conditions, students and teachers will experience either thermal discomfort or poor atmospheric comfort, both of which will negatively influence their ability to work and learn, affecting their overall well-being. Alternatively, the number of students per class would have to be severely limited (35 l/s corresponding to the ventilation demand for 15 students), which is not ideal. The recognized draught issue needs to be addressed in order to ensure optimal indoor comfort and welfare of the occupants.

## 3.2 Stage 2 - solutions

In this section, three different solutions addressing the issue of draught are explored:

1. Inlet design
2. Heater
3. Shelf system

To evaluate their potential, measurements on the whole grid of the measuring zone are performed (fig. 2.5). Building upon the conclusions drawn in the previous stage, only Fanger's model corrected for ankles is used in the analysis of the solutions (calculations using other models are provided in app. ch. C.3-C.5). All comparisons of draught rates are done for a border of the measuring zone ( $x = 1.5$ ) and for points 0.8, 1.2, 1.6 and 2 on Y axis. This is due to the observed influence of the door on the results, caused by high transmission losses and leakage (app. fig. C.33).

### 3.2.1 Step 1 - inlet design

This step investigates the effect of alterations to the inlet design on the active panel area, air velocity and draught rate. The changes to the inlet design are attained by sealing the gap between the Notech panel and the cover, which is placed 5 cm in front of the unit in the cold room. The experiments are conducted with three different sealing designs. In the first design, only the bottom is sealed off with tape. The second design is sealing off both the bottom and the right side (the opening side). The third design is sealing both sides and the bottom, leaving only the top open.

- Bottom sealed
- Bottom and right side sealed
- Bottom and both side sealed



These three design solutions are subjected to two different conditions, under which thermographic pictures are taken and values for air velocity, local air temperature and turbulence intensity are collected. The conditions are 12 dT and inlet opening of 33%, with the variable being the airflow, which in this case is either 35 l/s or 47 l/s. The specific conditions are selected because in stage 1 step 1 it was observed, that these conditions generate the least even use of the panel area. This makes it optimal when examining and assessing possible changes in the active panel area, air velocity and draught rate.

### **Results for the thermographic pictures**

The temperature gradient across the unit is determined and normalized the same way as in stage 1 step 1. The results for the three design solutions under the first condition setup (12 dT, 35 l/s, 33%) is shown in fig. 3.17 and the results for the design solutions under the second condition setup (12 dT, 47 l/s, 33%) is shown in fig. 3.18.

The fig. 3.17 and 3.18 show that similar trends are present in all the designs solutions. There is an almost uniform temperature for the three top sections and a drop in temperature from section 2 to the bottom - section 1. This is demonstrating that there is a mostly even air distribution throughout section 2–4, with a higher air distribution in the bottom section, as the temperature is still closer to the outdoor temperature here than in the rest of the panel. As all the design solutions shows similar results, it indicates that the area of restriction matters, rather than its specific location.

In connection with the bottom sealed design, an experiment with 100% opening of the inlet was also conducted, in order to investigate if the sealing also has an effect on the already more uniform area utilization that occurs at 100% opening. The result of this can be seen in app. fig. C.35. It shows that similar result is achieved as with the sealed 33% opening. There is therefore no further involvement of opening of 100%.

As the bottom sealing is showing a slightly more uniform temperature under the first condition (fig. 3.17) or similar result under second conditions (fig. 3.18), it is concluded that there is no reason to continue further work with the other design solutions. The bottom sealed design is also the simplest one and requires the least amount of adjustments to the original design.

12 dT, 35 l/s, 33%:

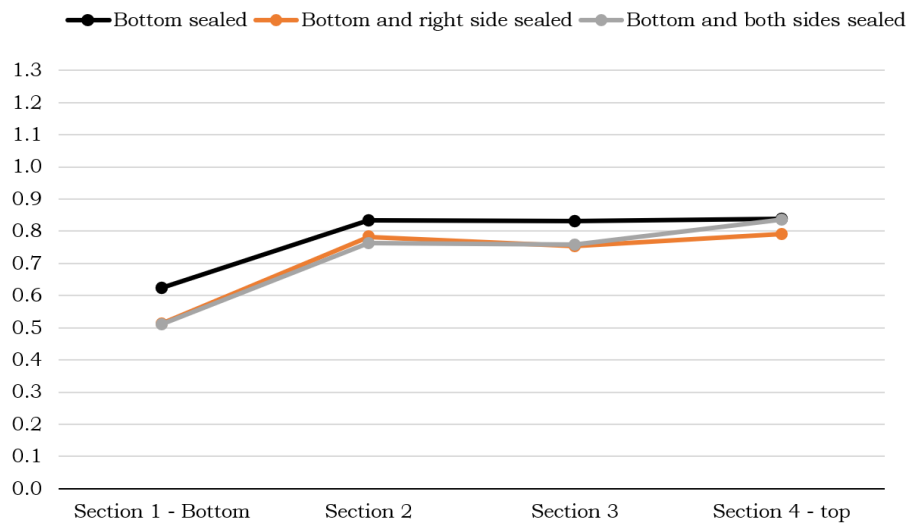


**Figure 3.17:** Comparison of temperature gradient across the panel under the conditions: 12 dT, 35 l/s, 33%, but with different sealing of the air intake

12 dT, 47 l/s, 33%:

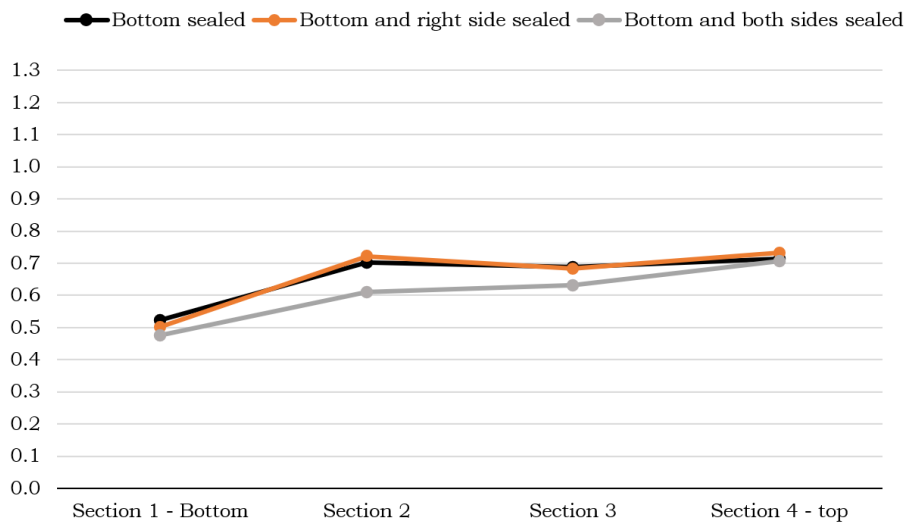


**Figure 3.18:** Comparison of temperature gradient across the panel under the conditions: 12 dT, 47 l/s, 33%, but with different sealing of the air intake

In fig. 3.19, a comparison between the bottom sealed design and the original inlet design under the first condition setup (12 dT, 35 l/s, 33%) is shown. Fig. 3.20 shows the same, just for the second condition setup (12 dT, 47 l/s, 33%). It must be noted that in stage 2, the methodology for achieving 12 dT between cold and hot room was changed. In the

stage 1, the hot room was heated up, however, in the stage 2, the hot room was kept at its current temperature and the cold room was cooled down to prevent high vertical temperature gradient in the hot room. This change in methodology might result in different temperature gradient values, therefore only the temperature distribution across the unit is used for comparison.

From fig. 3.19-3.20 it can be seen that the bottom sealing, has made the panel have a more even air distribution across the unit, compared with the original design. In that section 2-4 is more even, and the temperature drop to the bottom section has become smaller.

In fig. 3.19 this is shown in that the bottom sealed design in section 2-4, results in range of 0.84–0.82 and in section 2-1 0.82 - 0.63. Whereas in the original inlet design the values are in range of 0.73 – 0.62 and 0.62 - 0.32. The range between the section 2-4 is hereby 0.09 smaller and section 2-1 is 0.11 closer to each other.

Same trends are present in fig. 3.20. The bottom sealed design is in range of 0.71-0.69 in section 2-4 and from 0.70 to 0.52 in section 2-1. Whereas the original inlet is in range of 1.22 – 0.96 and from 0.96 to 0.60. The range between the section 2-4 is hereby 0.24 smaller and section 2-1 is 0.18 closer to each other.

**12 dT, 35 l/s, 33%:**

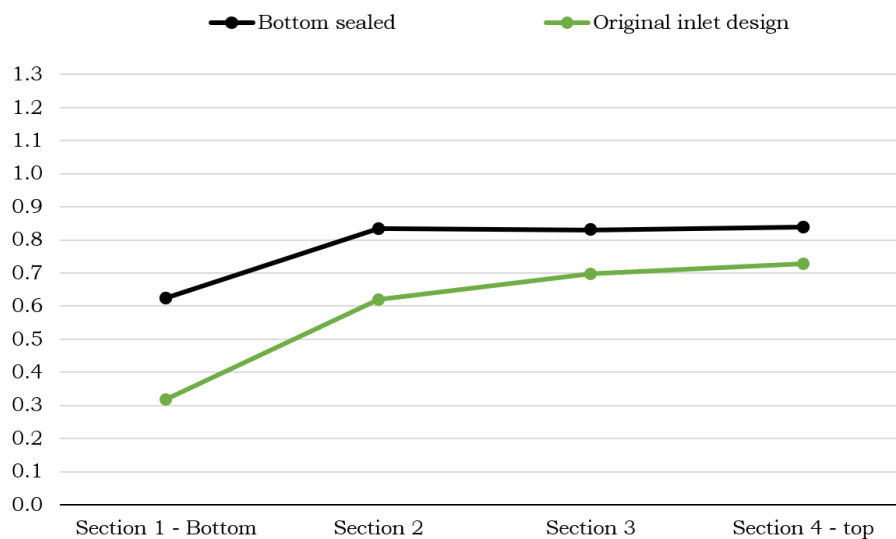


**Figure 3.19:** Comparison of temperature gradient between the original inlet design and the bottom sealed design, under the conditions: 12 dT, 35 l/s, 33%

12 dT, 47 l/s, 33%:

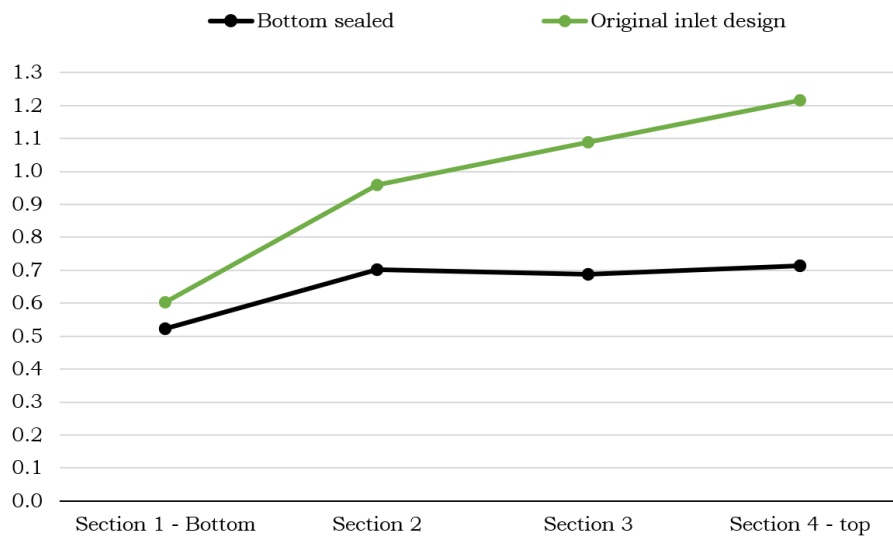


**Figure 3.20:** Comparison of temperature gradient between the original inlet design and the bottom sealed design, under the conditions: 12 dT, 47 l/s, 33%

### Draught

Fig. 3.21 compares draught results for the bottom sealed and original design under the conditions 12 dT, 35 l/s, 33%. The associated results for air velocity, local air temperature, turbulence intensity and draught following Fanger's and CBE formula is in app. fig. C.41 - C.49.

From the comparison, it can be seen that the bottom sealed design solution, with its more uniform air distribution across the panel, achieves a lower draught rate in all but one of the measurement points at the border. The one measurement point from the original design that achieves a lower value is the point at  $y=1.2$ . It has a rate of 11.15%, and the bottom sealed has a rate of 11.93%.

So the most critical point for the bottom sealed solution is in this case the area around the center of the panel. This is consistent with the results seen in stage 1 step 2. Based on that the measurements in that step were performed in the center in front of the panel and showed that the 100% opening, which has a more uniform air distribution across the panel than the 33% opening, have the highest draught rate at the last measurement point. This shows resemblance between the bottom sealed design solution and the original design.

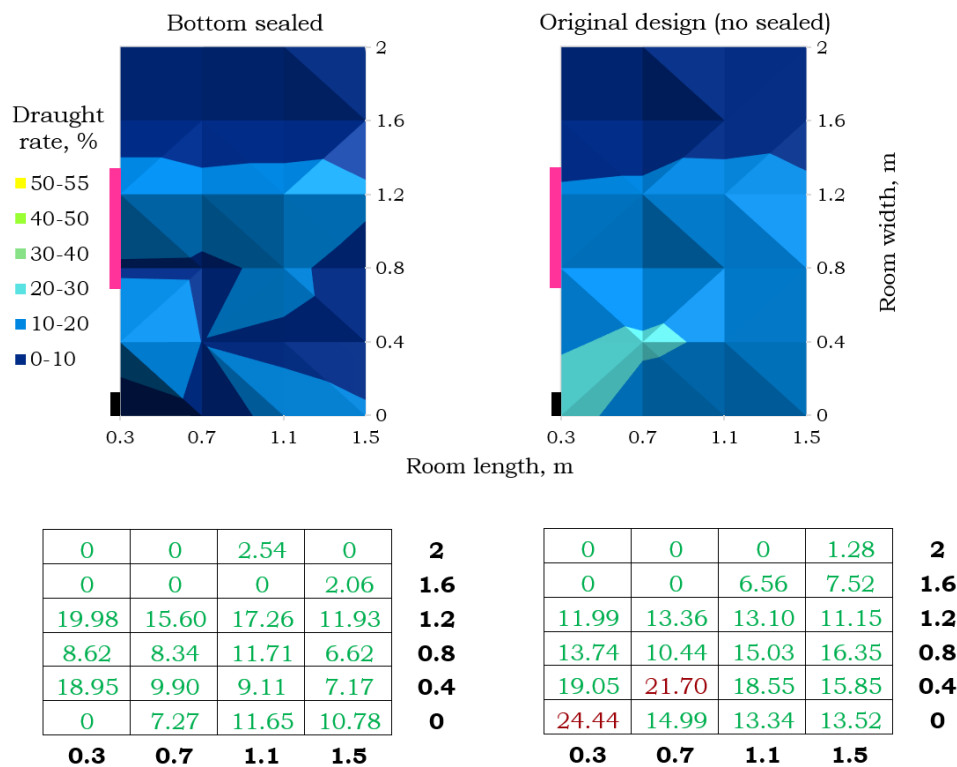


**Figure 3.21:** Comparison of draught rate at 12 dT, 35 l/s, 33% opening. Pink colour indicates position of the panel, and black of the door

### 3.2.2 Step 2 - heater

In this section of experiments a heater is implemented to evaluate its influence on the draught. The heater's power is set to 2000 W, which corresponds to calculated ventilation loss at the highest airflow and temperature difference or to 1000 W, which corresponds to 50% heat loss at 27 dT and 71 l/s. Due to inability to precisely control the heat source, a power of 1000 W is also used for lower airflows. See heat loss calculations for different air flows in app. fig. A.8.

In this stage the heater is placed right in front of the panel to see its maximum potential as a solution. The heated air from it interacts with the cold air, hence limits the amount of the air dropping to the floor and forcing it to mix with the air in the room and from the radiator instead.

During the first test, the radiator is placed on the floor and is subjected to the most critical conditions of 27 dt, 71 l/s, 100% opening of the inlet, as the previous measurements (ch. 3.1.2) show exceeding draught rates already at 47 l/s. As can be seen on the fig. 3.22,

this solution proves to be highly efficient, effectively eliminating the draught rate above 20%, not only on the border of the measuring zone (1.5 m from the panel), but also on the whole grid, allowing more space to be occupied. Moreover, evaluation with different draught models - Fanger (ISO 7730) and ASHRAE 55:2021, supports the findings. See app. ch. C.4 for all results for the heater.

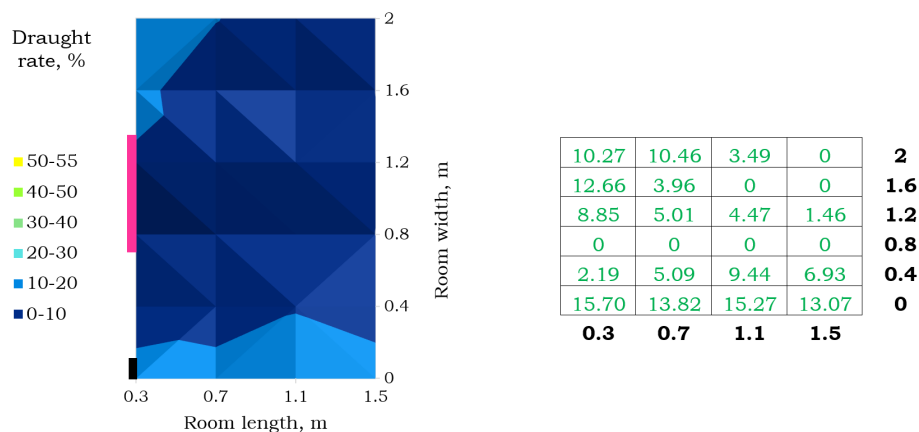


**Figure 3.22:** Draught rate at floor, 27 dt, 71 l/s, 100% opening, 2000 W. Pink colour indicates position of the panel, and black of the door

Comparison of two radiator positions (app. fig. A.7) is carried out, on the floor (fig. 3.23) and right underneath the inlet (fig. 3.24) under the following conditions: 71 l/s, 100% opening of the inlet and 1000 W. Based on these two figures it can be seen that the position of the radiator has an influence on the draught. When located on the floor, it helps with draught mainly in front of the panel, as the air is pushed to the sides. Location underneath the inlet makes the draught more distributed over the grid, therefore more area exceeds the allowed 20% limit. At the analysed points at the border, both heater positions can eliminate draught with 1000 W.

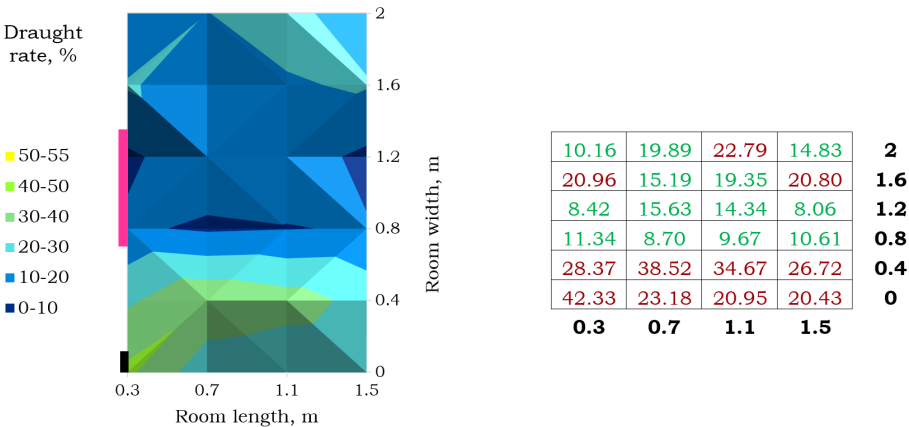


Figure 3.23: Draught rate at floor, 27 dt, 71 l/s, 100% opening, 1000 W. Pink colour indicates position of the panel, and black of the door

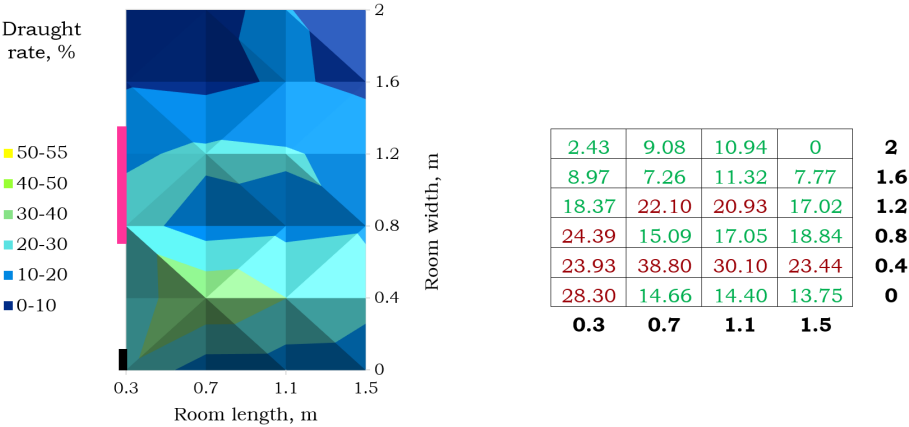


Figure 3.24: Draught rate under the inlet, 27 dt, 71 l/s, 100% opening, 1000 W. Pink colour indicates position of the panel, and black of the door

3.2.3 Step 3 - shelves

Shelf system is installed on the inner side of the panel to test its ability to reduce draught rate by posing a resistance to the flow thus reducing its velocity or by separating the flow and mixing with the room air. The flow behavior depends on the conditions, such as type of flow and the critical depth of the shelves. The exact critical depth is unknown, therefore the tested depth is chosen to be 30 cm as for turbulent flow under transient conditions [14].

The system consists of 5 shelves – one right under the window opening and the other 4 evenly distributed along the height of the panel. The width of the shelves corresponds to the width of the panel. The experiments were performed in 3 variations:

1. Solid shelves
2. Solid shelves with edges
3. Perforated shelves with edges

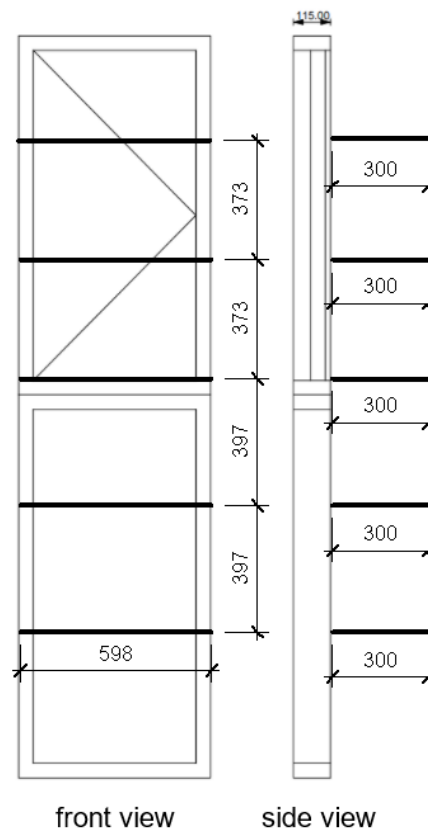


**Figure 3.25:** Front and side view of the 5 shelf system design



### Solid shelves

The experiments were performed under 22 dT as measurements from the stage 1 start to show problems with draught at this temperature difference and the air flow of 47 l/s. Fig. 3.27 shows DR under 22 dT, 47 l/s and 33% opening. The unacceptable rates are only exceeded in the bottom right corner. This is due to the low air temperature in the that zone as the velocity and turbulence intensity are relatively similar on the border (see velocity, air temperature and turbulence intensity graphs in app. fig. C.87 - C.89). The same conditions are tested with a 100% opening, showing higher velocity throughout nearly the whole measured zone, resulting in higher draught rates. Lastly, the solid shelves system is tested under the highest flow of 71 l/s and 100% opening. The measurements show similar results along the border of the near zone – the draught rate is exceeded by maximum of 3.43%.

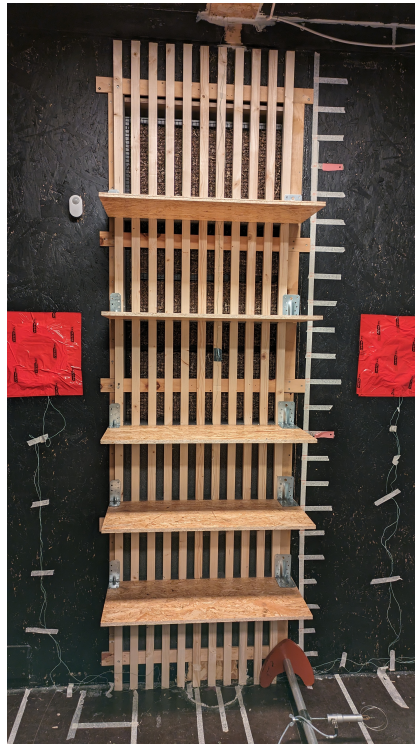


**Figure 3.26:** Picture of the solid shelves

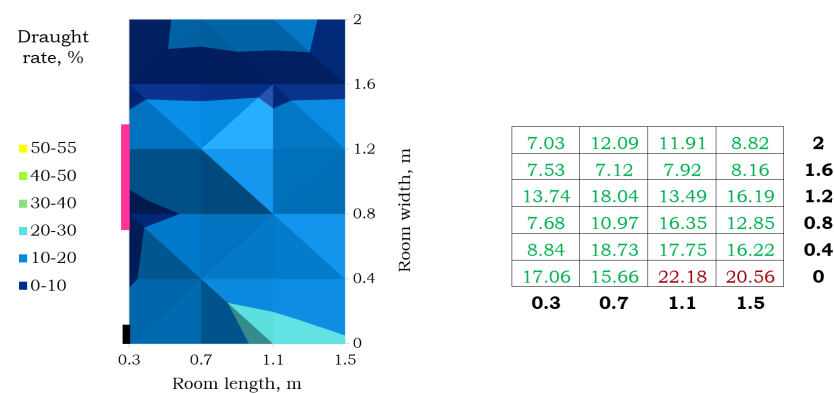


Figure 3.27: Draught rate at 22 dT, 47 l/s, 33% opening. Pink colour indicates position of the panel, and black of the door

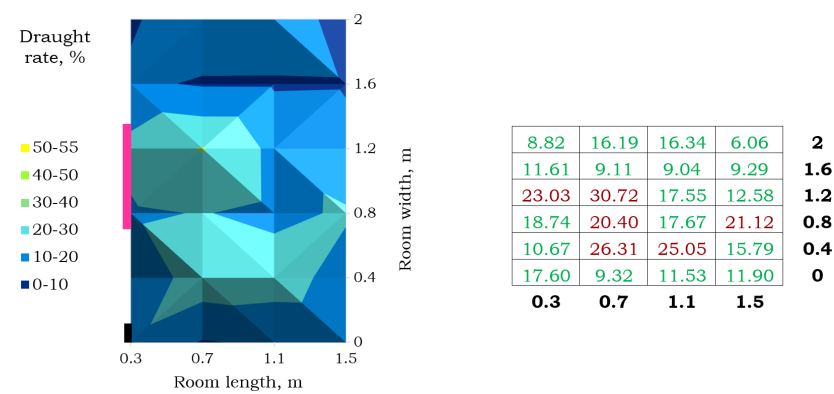


Figure 3.28: Draught rate at 22 dT, 47 l/s, 100% opening. Pink colour indicates position of the panel, and black of the door

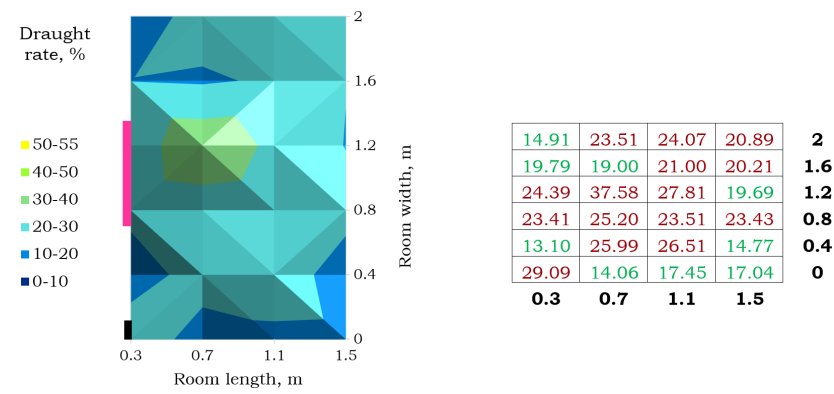


Figure 3.29: Draught rate at 22 dT, 71 l/s, 100% opening. Pink colour indicates position of the panel, and black of the door

### Solid shelves with edges

The shelf system was altered by installing an additional vertical resistance to enhance mixing – 5 cm edge at the end of each shelf. The measurements were performed under 22 dT and 47 l/s as the solid shelves to compare the impact of this alteration. Moreover, the 22 dT, 71 l/s and 33% was also tested to find a limit of this solution. The draught starts to exceed acceptable limits at 22 dT, 47 l/s and 100% opening. However, this exceed is moderate (21.09%) and is assumingly caused by the door (app. fig. C.107). The highest velocity levels occur in proximity to the door, leading to elevated DR in this specific area. This region becomes particularly critical at the maximum air flow of 71 l/s, with the DR peaking at 24.36%.

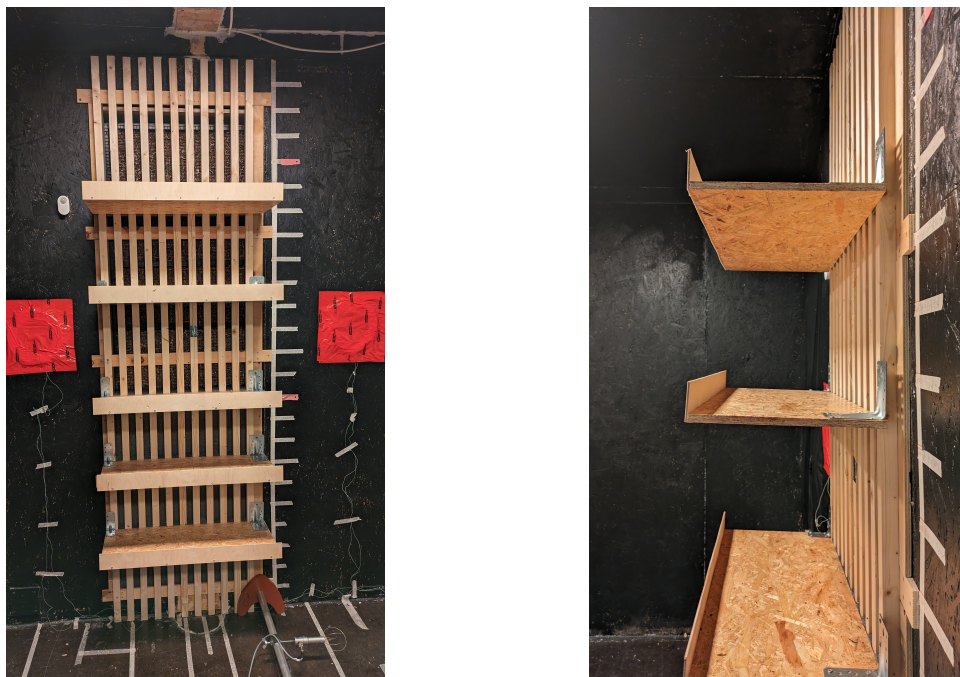


Figure 3.30: Picture of solid shelves with edges

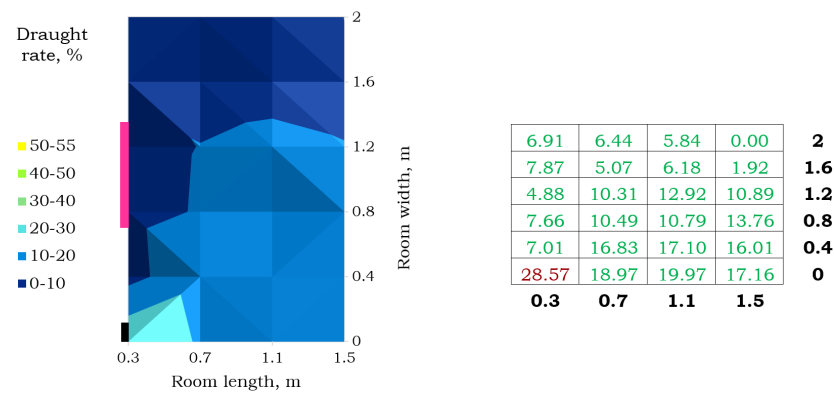


Figure 3.31: Draught rate at 22 dT, 47 l/s, 33% opening. Pink colour indicates position of the panel, and black of the door

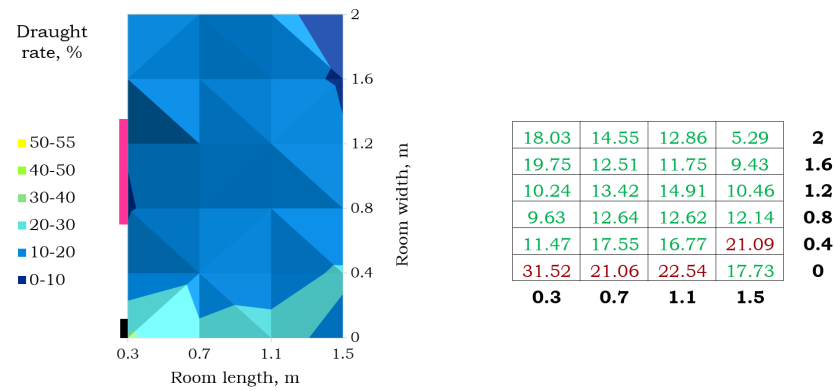


Figure 3.32: Draught rate at 22 dT, 47 l/s, 100% opening. Pink colour indicates position of the panel, and black of the door

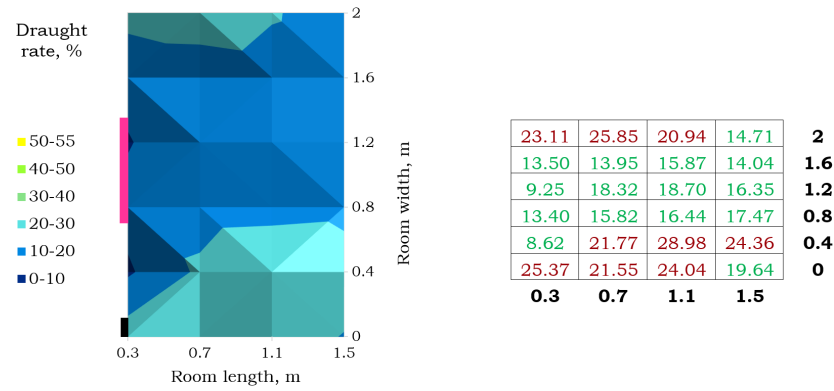


Figure 3.33: Draught rate at 22 dT, 71 l/s, 33% opening. Pink colour indicates position of the panel, and black of the door

### Perforated shelves with edges

In the last alteration of the five piece shelf system, solid shelves are changed to perforated ones. The vertical edge is kept. The aim of this proposal is to allow some of the air to penetrate down through the shelves. By doing this, the underpressure built up under the shelf is partially released and the air coming around the shelf is not forced to reattach to the wall with as high force as with the solid shelves. The measurements are performed under same conditions as solid shelves.



Figure 3.34: Picture of perforated shelves with edges

Similarly to previous results, the draught does not exceed unacceptable limits with airflow of 47 l/s, if point in front of the door is disregarded. At 71 l/s, the draught limit is exceeded in several points, however this increase is again very moderate and is within the expected error margin.

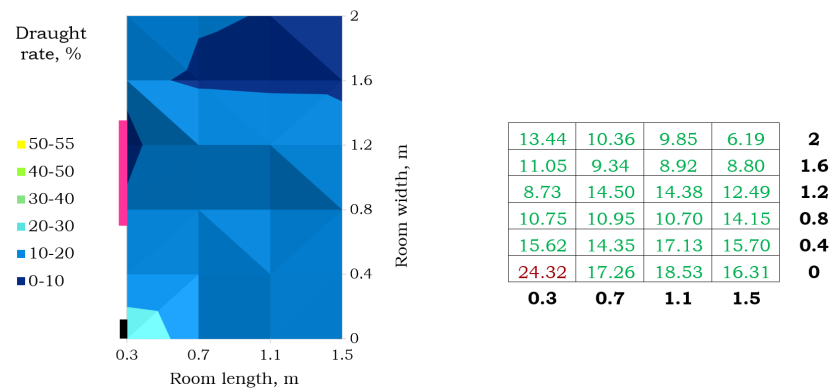


Figure 3.35: Draught rate at 22 dT, 47 l/s, 33% opening. Pink colour indicates position of the panel, and black of the door

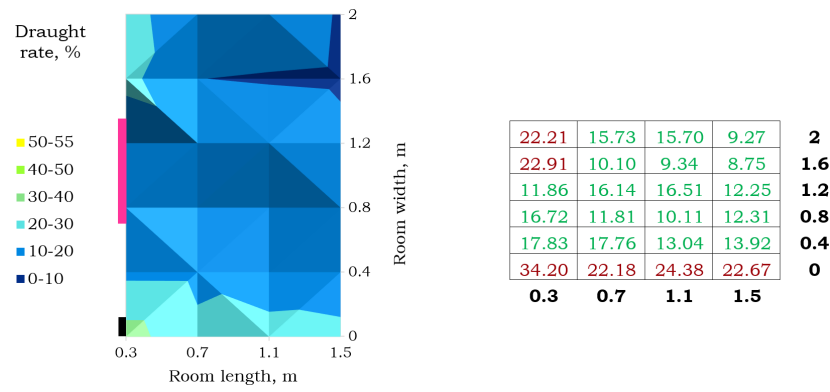


Figure 3.36: Draught rate at 22 dT, 47 l/s, 100% opening. Pink colour indicates position of the panel, and black of the door

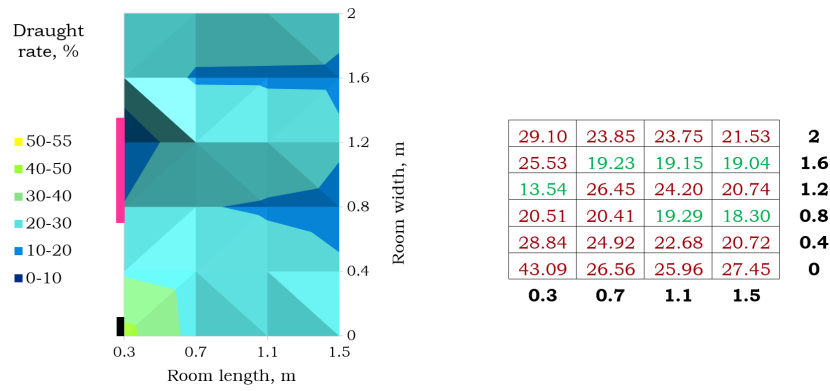


Figure 3.37: Draught rate at 22 dT, 71 l/s, 100% opening. Pink colour indicates position of the panel, and black of the door

### Single shelf with edge

In addition to the experiments with varying shelf types, it was also investigated if reduction in the amount of shelves can achieve better/equal results in lowering draught rate. The amount of shelves is changed from five to one shelf. The remaining shelf is placed right under the active panel part opening. The "single shelf" design can be seen in app. fig. A.14. The implemented variation of shelf is the perforated shelf with edge. The "single shelf" design is subjected to the same conditions that were used with the perforated shelves with edge.

In fig. 3.38 the draught rate comparison between five and one shelf is shown for the conditions 22 dT, 47 l/s and 33% opening. From this comparison it can be concluded that one shelf can achieve similar reductions in draught rate as the five shelves; based on that the results at the border are almost identical. The average value at the border for five shelves is 10.41% and for one shelf it is 11.64%.

The draught rate comparison between five and one shelf under the conditions 22 dT, 71 l/s and 100% opening can be seen in app. fig. C.152. Average value at the border for five shelves is 19.90% and for one shelf it is 16.21%. Therefore showing the same pattern, in that the one shelf can achieve comparable results to the five shelves.

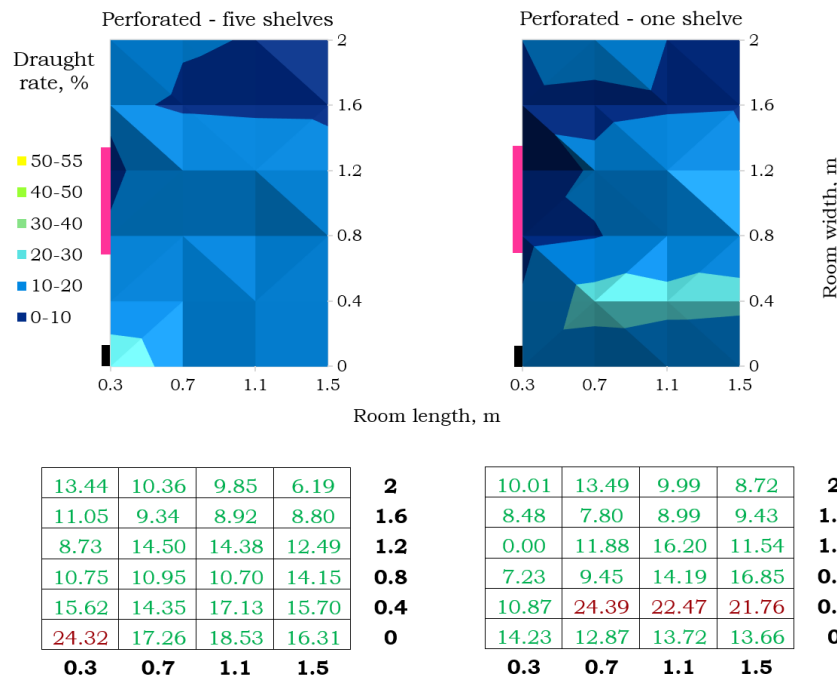


**Figure 3.38:** Comparison of draught rate for five and one perforated shelves - 22 dT, 47 l/s, 33% opening. Pink colour indicates position of the panel, and black of the door

**Summary**

The results of the measurements show that the shelf system has a positive effect on the draught in the near zone. The solid shelves show the smallest ability to reduce draught, however they still improve the rates in comparison with the original design. The limit for the solid shelves is at 22 dT and 47 l/s, however the DR limits are exceeded only slightly.

Adding an additional resistance in form of a vertical obstacle showed improved rates in all measured conditions in comparison to the solid shelves. The edges seem to push the air to the sides causing the most critical regions to be in the corners of the near zone, not in front of the panel. The limit is reached at the highest air flow of 71 l/s where the DR limit is exceeded at one spot at the door side of the measured zone. The last solution with perforated shelves shows similar results at 47 l/s as the solution with solid shelves and the edge. At higher airflow, the limit is exceeded only moderately and therefore this solution is considered sufficient at 22 dT.

Since the last two versions of the shelf system, solid with edge and perforated with edge, show nearly identical results, it is recommended that a more feasible solution of these, in terms of economy and material resources, is chosen for further design. With the aim of material savings, a shelf system with only one shelf is tested. The measurements show that similar results can be achieved with using just one shelf. The depth of the shelves is chosen based on assumptions of the flow characteristics - it is not known to what extent this depth causes the air to separate or just pose a resistance. A reduced shelf depth should be investigated as it might bring similar results as the chosen depth.

**3.2.4 Step 4 - combined solution of shelves and heater**

Perforated shelves and heater combination is proposed as one of the possible solutions. The perforations are thought to allow for more uniform rise of heat and therefore mitigating formation of convection currents, which can contribute to thermal discomfort. As shelves are a passive solution for draught, it is investigated if they are sufficient in conjunction with smaller power of the heater (1000 W instead of 2000 W), hence minimizing the energy consumption. Moreover, comparison between 1 and 5 perforated shelves in connection with heater is performed to ensure that their performance is aligned with conclusion in ch. 3.2.3.



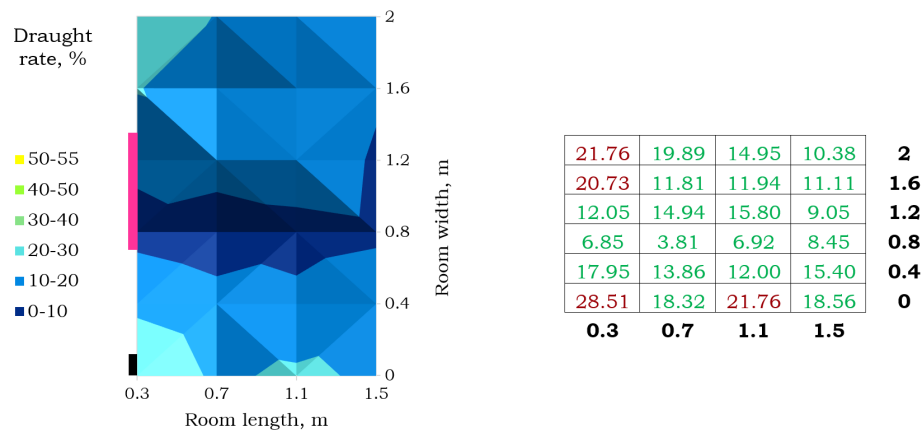


**Figure 3.39:** Draught rate for five perforated shelves with edge and heater - 27 dT, 71 l/s, 100% opening, 1000 W. Pink colour indicates position of the panel, and black of the door

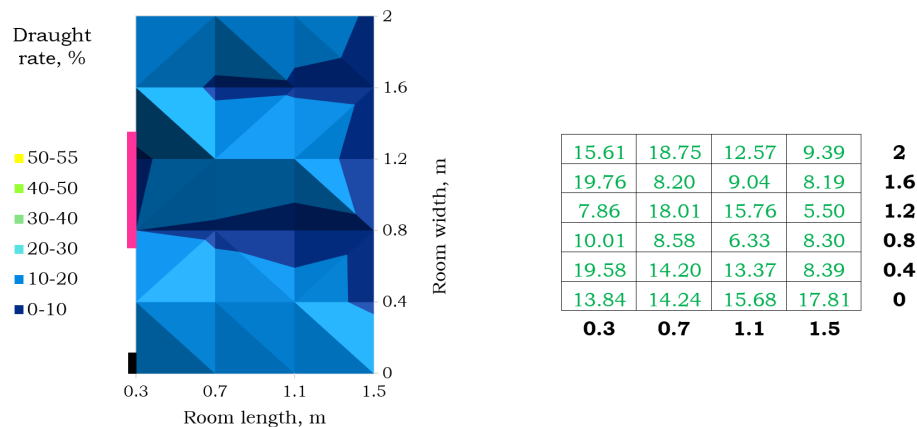


**Figure 3.40:** Draught rate for one perforated shelf with edge and heater - 27 dT, 71 l/s, 100% opening, 1000 W. Pink colour indicates position of the panel, and black of the door

The fig. 3.39-3.40 showcase the effectiveness of combining these two solutions under the most critical conditions - highest temperature difference of 27 dT and airflow of 71 l/s. As demonstrated by individual experiments (subch. 3.2.3), a shelf system solution fails to fully address the problem. However, together, they successfully eliminate the draught across most of the grid, allowing more area of the room to be occupied. The number of perforated shelves appears to have minimal influence on the results, making one shelf a recommended and more feasible solution.

See a comparison of draught rates under original conditions and new proposals in app. fig. C.153.



## Chapter 4

# Conclusion

To conclude, this paper investigates draught for a new sustainable ventilation concept, the Notech panel, and proposes solutions for its improvement. The research questions are answered through conduction of experiments on the prototype in a laboratory setting.

### **1. What is the current performance of the Notech panel regarding the inlet opening activity?**

Air distribution through the filter was investigated using thermographic camera. The measurements showed that the air behaves similarly under different temperature differences. However, increasing airflow and opening have a more significant effect. The higher the airflow, the more even distribution through the panel. Similarly with opening of the inlet, where at 100% opening, the air movement through panel is more uniform than at 33%. Despite more even distribution in these instances, most of the air still penetrates through the bottom section of the panel. These findings were used in exploring the solutions and could benefit future adjustments in panel design.

### **2. What are the current draught rate limits and how does the position of the venting opening influence the draught rate?**

The draught rate limits were found using three different models. For 12 dT, the acceptable limit is only exceeded at the highest of the investigated airflows with one of the models. At 22 dT, the limit was reached at 47 l/s and 33% opening with all three models. The same limit is expected for 27 dT. It was found that lowering the original panel position does not have a positive effect on the draught rates, therefore the study continued with the original panel height.

### **3. How does the choice of draught model impact the interpretation of results?**

Three different draught models were used to investigate percentage of dissatisfied with draught. The broadly used draught model from ISO 7730 overestimates results as it is

designed for the neck area. As this study focused on draught at ankle height, the corrected Fanger's formula is used as a second model. Lastly, a more complex CBE comfort tool is used which requires more measured and assumed inputs. However, this tool has a limitation in clothing level of 0.7 clo, which is not considered to be enough for the studied winter case. Therefore, it is concluded that the most suitable model for this study is Fanger's corrected model for ankles.

#### **4. What solutions could be implemented with Notech prototype to extend the limits of the panel regarding the draught rate?**

The study explored both shelf systems as a passive solution, and a heater as an active solution for the draught issue. It was concluded that the heater solution is the most effective in combating the draught, however, also the most energy consuming. With a power that corresponds to 50% heat loss from ventilation, the draught can be fully eliminated at the most critical conditions tested.

The shelf system was tested in different variations. All of the tested alterations have a positive effect on draught rate. A system of 5 shelves with edges showed to have a similar effect as only one shelf, with a limit at 22 dT. The depth of the shelves should be investigated further as more narrow shelves might also bring satisfactory results. As the passive solutions failed to address the draught issue under the most critical conditions, the heater and perforated single shelf solutions were combined, resulting in successful draught elimination. For the aim of further energy savings, the minimum required heater power needs to be found.

# Bibliography

- [1] WindowMaster International A/S. *Notech mmeeting with AAU*. Unpublished Power-Point presentation. 12.09.2023.
- [2] Danish Standard Association. *DS/EN ISO 7730: Ergonomics of the thermal environment - analytical determination and interpretation of thermal comfort using calculation of the PMV and PPD indices and local thermal comfort criteria*. 2st. Danish Standard Association, 2006.
- [3] Danish Standard Association. *DS/EN ISO 9972:2015*. 1st. Danish Standard Association, 2015.
- [4] Danish Standard Association. *EN 16798-1 2019: Energy performance of buildings – Ventilation for buildings – part 1: indoor environmental input parameters for design and assessment of energy performance of buildings addressing indoor air quality, thermal environment, lighting and acoustics – Modul M1-6*. 1st. Danish Standard Association, 2019.
- [5] European Comission. *Factsheet: Buildings (European Green Deal package December 2021). MAKING OUR HOMES AND BUILDINGS FIT FOR A GREENER FUTURE*. 2021. URL: <https://t.ly/AK5d2>. (accessed: 23.09.2023).
- [6] Metric conversions. *Millimeters of water to Millibar*. October 23, 2023. URL: <https://www.metric-conversions.org/pressure/millimeters-of-water-to-millibar.htm>. (accessed: 23.10.2023).
- [7] TLK Energy. *Air density: calculate the density of air*. October 23, 2023. URL: <https://www.metric-conversions.org/pressure/millimeters-of-water-to-millibar.htm>. (accessed: 23.10.2023).
- [8] Hanzawa H et al Fanger PO Melikov AK. *Air turbulence and sensation of draught*. Energy and buildings, 1988. Chap. 12.
- [9] M. Frandsen. *Exercise 1.9.1 calibration of anemometers*. 2022.
- [10] Refrigerating American Society of Heating and Air-Conditioning Engineers. *ASHRAE Standard 55-2020, Thermal Environmental Conditions for Human Occupancy (ANSI Approved)*. 1st. American Society of Heating, Refrigerating, and Air-Conditioning Engineers, 2020.

- [11] Danish technological institute. *A:Notech eelgrass filter collection of temperaturecorrected results from the indoor climate laboratory*. Danish technological institute, 2023.
- [12] Danish technological institute. *Test of the Notech eelgrass filter air intake located in external facade – used as displacement armature in school*. Danish technological institute, 2023.
- [13] K. B. Johannsen T. Ø. M. K. Sørensen og M. D. A. Andersen M. H. Vorre P. N. S. E. Maagaard. *Industry guidance for indoor climate in schools*. Technological Institute, 2021.
- [14] E. Bjørn P. Heiselberg H. Overby. *The Effect of Obstacles on the Boundary Layer Flow at a Vertical Surface*. Dept. of Building Technology and Structural Engineering, 1994.
- [15] Building Ministry of Transport and Housing. *Executive order on building regulations (BR18)*. 2018.
- [16] C. Volf et al. *Energy-efficient renovation of schools: Daylight, natural ventilation, and natural materials. Results from a pilot study: NOTECH solution vs. mechanical ventilation*. Elforsk, 2021.
- [17] WindowMaster. *The key to sustainable buildings. Why and how to use natural ventilation in your building design*. URL: <https://t.ly/1n0zw>. (accessed: 19.09.2023).